5-1984

Corrosion of Carbon Steel in Synthetic Coal Liquid Wash Waters

Keith Evans
Western Kentucky University

Evans,

Keith D.

1984

CORROSION OF CARBON STEEL IN SYNTHETIC COAL LIQUID WASH WATERS

A Thesis

Presented to

the Faculty of the Department of Chemistry

Western Kentucky University

Bowling Green, Kentucky

In Partial Fulfillment

of the Requirements for the Degree

Master of Science

by

Keith D. Evans

May 1984

AUTHORIZATION FOR USE OF THESIS

Permission is hereby

☒ granted to the Western Kentucky University Library to make, or allow to be made photocopies, microfilm or other copies of this thesis for appropriate research or scholarly purposes.

☐ reserved to the author for the making of any copies of this thesis except for brief sections for research or scholarly purposes.

Signed Keith D. Evans

Date 5/30/84

Please place an "X" in the appropriate box.

This form will be filed with the original of the thesis and will control future use of the thesis.

CORROSION OF CARBON STEEL IN SYNTHETIC

COAL LIQUID WASH WATERS

Recommended May 2, 1984
(Date)

Lawrence J Bouchard
Director of Thesis

John T. Riley

Burton H. Davis

R Leggett

Approved June 1, 1984
(Date)

Edmund Troy
Dean of the Graduate College

DEDICATION

I dedicate this thesis to my loving parents Morris and Faye Evans whose encouragement and support throughout my life have enabled me to achieve this goal, and to Carol Clark for her endless patience and friendship.

ACKNOWLEDGEMENTS

I wish to acknowledge my most sincere gratitude to the faculty of Western Kentucky University's Chemistry department, particularly Dr. Laurence J. Boucher and Dr. John T. Riley for their guidance in the completion of this thesis and to Dr. Burtron H. Davis and Dr. Alberto A. Saques for their help in gathering the data.

CORROSION OF CARBON STEEL IN SYNTHETIC COAL LIQUID WASH WATERS

Keith D. Evans May 1984 77 pages

Directed by: Laurence J. Boucher, Burtron H. Davis, Alberto A. Sagues, and John T. Riley.

Department of Chemistry Western Kentucky University

The Potentiodynamic corrosion measuring technique is an electrochemical analytical method which measures corrosion rates of a metal exposed to a corrosive environment.

The corrosion characteristics of carbon steel M1044 in aqueous solutions of aniline hydrochloride,simulating a coal liquid wash water, were determined by this method. The effects of solution velocity and oxygen concentration on the system were also determined.

A bimodal corrosion rate effect was observed in deaerated solutions of 1000 and 5000 ppm chloride as aniline hydrochloride. This effect was interpreted to be the result of the formation of a film on the surface of the specimen.

TABLE OF CONTENTS

LIST OF FIGURES

LIST OF TABLES

INTRODUCTION

The United States' dependence on foreign oil supplies has led to several energy crises which have spurred interest in the development of an alternate energy technology. It has been recognized that a domestic energy supply is critical to the United States' economy and that utilization of our coal supplies, which comprise 27 percent of the world's known coal reserves, is of paramount importance.(1)

One of the areas of research in coal utilization is the development of a synthetic liquid fuel technology. To this effect, several multi-ton coal liquefaction plants have been constructed in the United States within the last decade. As with any new technology, several unexpected problems were encountered. One of the more serious problems has been severe corrosion in the fractionation area of these platns, which has been attributed to the formation of corrosive amine hydrochlorides in the process liquids.(2) Chloride enters the process as a minor constituent of the feed coal.(3)

Several corrosion prevention schemes have been suggested. One of these is water washing of the process liquids to remove the water soluble amine hydrochlorides.(4) The problem then becomes processing of the highly corrosive wash waters.

Therefore, an understanding of corrosion in synthetic coal liquid wash waters would be useful in the design of wash water areas of a coal liquefaction plant.

In this study, the corrosion characteristics of carbon steel in a synthetic coal liquid wash water were determined. In order to characterize a corrosion system, a corrosion measuring technique must be utilized which will enable rapid and accurate measurements. The conventional weight loss method of corrosion monitoring is too cumbersome and time consuming for this type of study. For these reasons, the electrochemical potentiodynamic technique was employed. The purpose of this project was to investigate the corrosive properties of a synthetic coal liquid wash water by the potentiodynamic method and thus gain valuble information to aid in the design of wash water processing areas of commercial coal liquefaction plants.

BACKGROUND

Within the last decade several multi-ton coal liquefaction pilot plants have been constructed in the United States. Severe corrosion problems have been encountered in the fractionation area of these plants which is uncommon in petroleum refinement systems. Severe corrosion occured in the fractionation area of both solvent refined coal (SRC-1) plants in Wilsonville, Alabama, and Fort Lewis, Washington.[5,6] Corrosion rates exceeding 1000 mils per year were detected by means of resistance type corrosion probes within narrow regions of the atmospheric distillation tower at the Wilsonville plant. One mil per year is equivalent to 0.001 inch per year. Corrosion was so severe that the tower was decommisioned and relined after only six months of operation.

Operators of the solvent refined coal pilot plant in Wilsonville, Alabama, identified chlorine in the feed coal as the corrosive component.[3] They also found that additions of sodium carbonate to the feed coal could reduce corrosion to acceptable levels; however, this technique is not directly applicable to commercial plants for several reasons.[7] First, it is neither practical nor economical to add the amount of sodium carbonate required for a commercial plant. Second, high sodium containing compounds

cannot be fed to existing gasifiers that produce the hydrogen required for the process. Thus, another solution to the problem needs to be determined.

Since chloride was identified as the corrosive component of the system, several questions concerning the nature and pathway of the chloride needed to be answered.[4]

1. What is the chemical form of the corrosive chlorides?
2. What is the pathway of the chloride through the distillation area?
3. Why does corrosion occur exclusively in the last tower of the distillation process rather than in some previous vessel?
4. Why is corrosion localized in certain areas of the tower?
5. What problems are encountered in implementing steps to reduce the corrosion?

It was first thought that the chemical form of the chloride was a naphthenic acid compound which has been found to cause corrosion in petroleum refinement. Subsequent investigations indicated that this was not a likely mechanism.[8] Analysis of samples from the Wilsonville SRC-I plant revealed that the major portion of chloride was in a water-soluble form.[9] The pathway of the corrosive chlorides in the Wilsonville SRC-I plant was elucidated from chemical analysis of samples taken at various points from the process stream.[7] Figure 1 is a schematic illustrating portions of the SRC-I process. The general pathway was found to be as follows. Chloride enters the process as a minor component of the feed coal. The

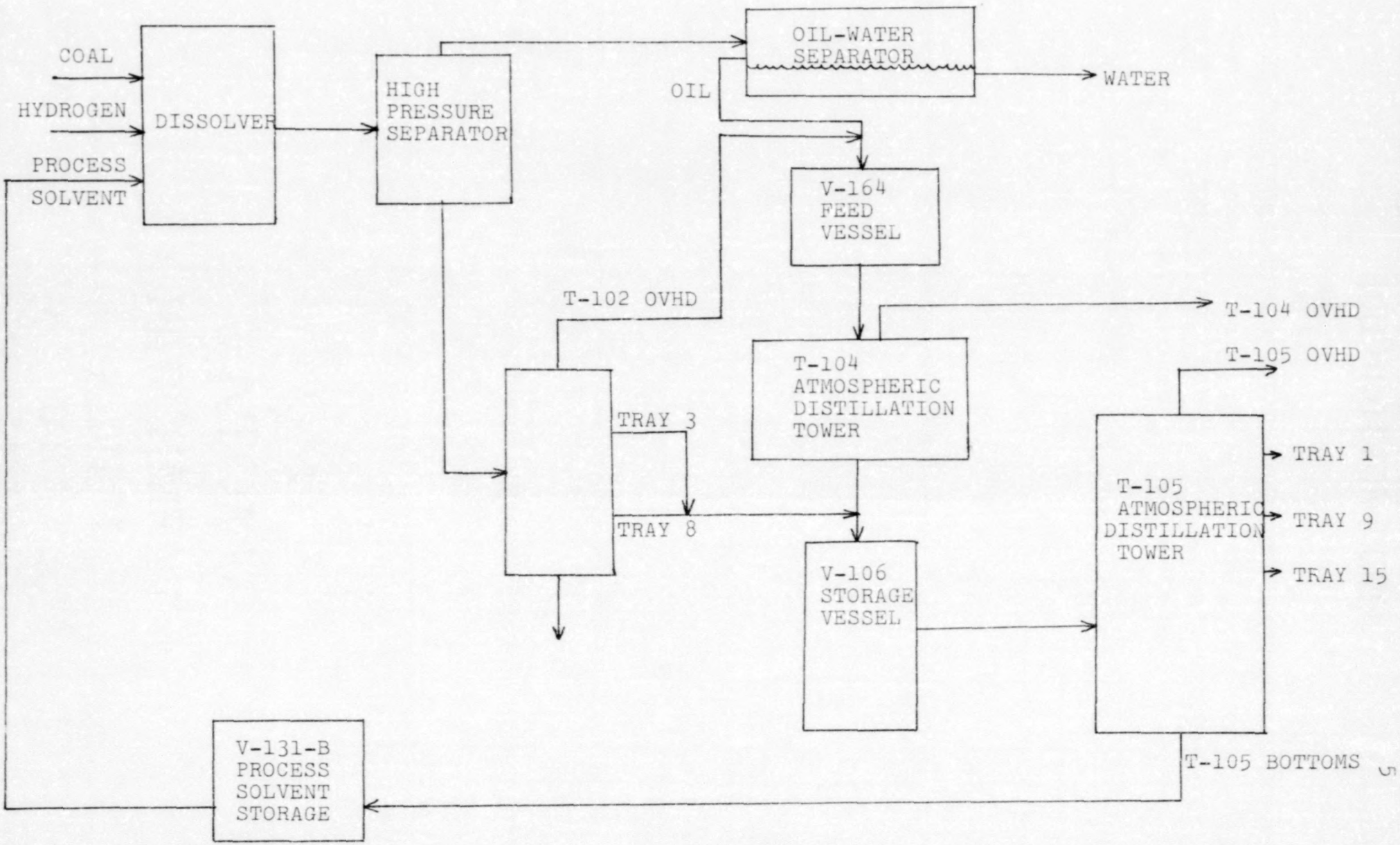

Figure 1. Wilsonville Alabama Solvent Refined Coal SRC-I process schematic.

chloride is concentrated in the dissolver, due to retention in the process solvent, to a high steady-state chloride concentration. The process liquids leaving the dissolver are separated in a high pressure separator, then exit in two streams: overhead and bottoms. The overhead stream from the separator is cooled and allowed to settle in a storage vessel into organic and aqueous phases, the latter of which contains the water soluble chlorides. The chloride from the overhead is removed from the process at this point. The majority of the chloride, however, exits the separator in the bottoms stream. This stream is fed into the vacuum distillation tower T-102 where it is separated into chloride-containing solids and liquids. The chloride-containing solids leave the process at this point. The chloride-containing distillate stream from T-102 is then fed into the atmospheric distillation tower T-105 via the V-106 storage vessel.

It was in the T-105 tower that corrosion was found to be most severe. One might wonder why the vacuum distillation tower and other vessels in the process prior to T-105 did not have corrosion problems, since the process stream in these vessels also contained the corrosive chlorides. An explanation for this can be found in the solubility of the chlorides in the various process streams.(2)

It was determined by chemical analysis of samples that the SRC-I pilot plant liquids were composed of acidic, basic, and neutral fractions. The acidic fraction was composed mainly of phenols and the basic fraction of various amines. Laboratory experiments revealed a synergistic effect

of the chlorides, phenols, and amines which enhanced and localized corrosion in the T-105 tower.[2] The water soluble chloride was found to be highly corrosive when present with basic nitrogen-containing compounds but fairly uncorrosive when these compounds were not present. It was determined that the corrosivity was due to amine hydrochlorides which formed in a reaction with water soluble chlorides and amines. Furthermore, the phenolic fraction provided a more polar solvent for the amine hydrochlorides and therefore retained them in solution. In the absence of phenols, the amine hydrochlorides distill out of solution. This synergistic effect provides a mechanism for concentration of the corrosive amine hydrochlorides in localized regions of the process. An equilibrium is eventually reached in the fractionation tower where the amine hydrochlorides are sufficiently soluble in the process liquid to accumulate in high concentrations.[7] It is at these equilibrium regions that corrosion was most severe. This mechanism provides a role for inorganic chloride, basic nitrogen compounds, phenols, and temperature in the localized corrosion.

Analysis of Wilsonville SRC-I liquids and laboratory experiments revealed that the corrosion was a chemical reaction with chloride rather than catalytic.[2] Laboratory corrosion rates of steel coupons immersed in the plant liquids in a closed system showed that corrosion decreases with time through a stochiometric consumption of chloride. The data also implied a product formation of ferrous chloride, $FeCl_2$.

Attempts to Allevaite Corrosion Problems

Several corrosion prevention schemes have been suggested which are composed primarily of either 1) preventing concentration build up of chloride in the affected area or 2) changing the chlorides to a less corrosive form or 3) using more corrosion resistnat alloys.[4] It is probable that a combination of these will eventually be implemented. Each scheme has advantages and disadvantages when the overall process is considered. As was mentioned previously, additions of sodium carbonate to the feed coal would effectively prevent buildup of chlorides by removing them from the process stream; however, this would not be a viable solution in commercial plants.

One of the more acceptable schemes is water washing of the process liquids to remove the water soluble chlorides. In the oil-water separation of the high pressure separator overheads most of the corrosive chlorides were removed from the process in the aqueous phase, thus suggesting that water washing of the process stream may be a solution to the problem. Unfortunately, the bottoms of the high pressure separator contained the major portion of the chlorides, and cooling and reheating of the bottoms stream for water washing may not be economical. Furthermore, the density of the liquid is very similar to that of water and, thus, may create separation problems.[2] In any event, water washing of the process liquids seems to be at least a part of the eventual solution to the problem.

The water wash scheme was the impetus for an investigation of corrosion in synthetic coal liquid wash waters. Analysis of T-105 process liquids determined that the largest percentage of the amines present were weak bases such as pyridines, quinolines, and anilines.[2] Aniline hydrochloride was chosen for a synthetic wash water system since it is representative of those amine hydrochlorides expected to be present in the wash waters.[7] Weight loss corrosion experiments were performed in 1000 ppm aqueous chloride solutions of aniline hydrochloride at boiling and room temperatures.[4] Initial corrosion rates of carbon steel in the boiling solution approached 10,000 mils per year and then tapered off to background levels. Corrosion in the room temperature solution was still above acceptable levels, thus indicating the highly corrosive nature of the solution. Results of experiments conducted to determine the response of other alloys to the aniline hydrochloride solution are shown in Figure 2.[4] The stainless steels appeared to be much more corrosion resistant than carbon steel during the time interval of the tests;and,thus, the use of these materials to combat corrosion in the affected areas is promising. An in-depth investigation of corrosion in aqueous solutions of aniline hydrochloride would yield valuable information to the design of wash water areas of commercial plants.

Potentiodynamic Technique for Measuring Corrosion Rates

The potentiodynamic technique was utilized for corrosion measurements in the aqueous aniline hydrochloride system

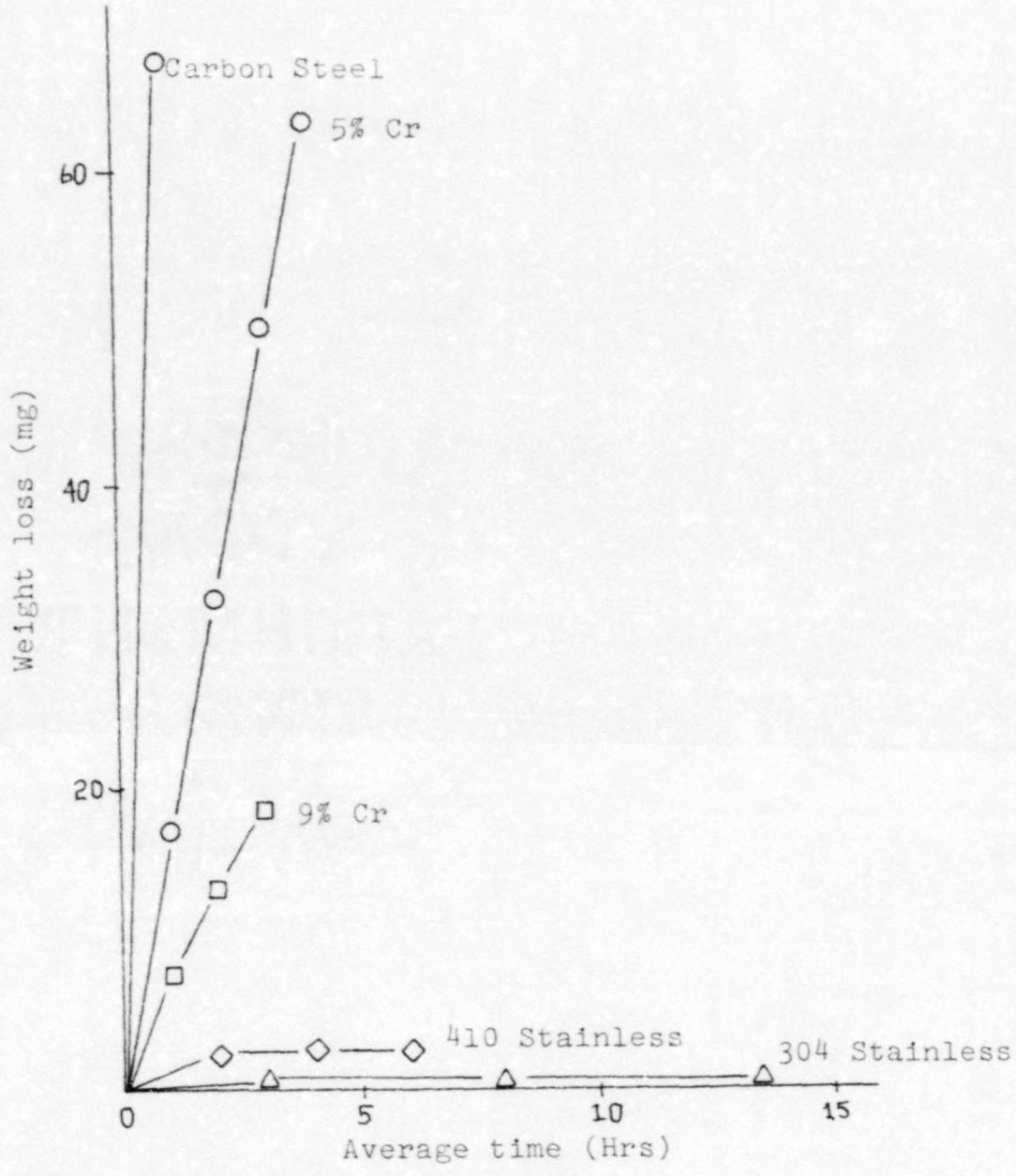

Figure 2. Alloy response in 1000 ppm aqueous aniline hydrochloride at boiling point.(4)

since it is a more rapid technique than the conventional weight loss method and measures instantaneous, as opposed to average, corrosion rates. In addition, the potentiodynamic method is capable of measuring extremely low corrosion rates which would require days or weeks to measure by weight loss.[10] Any explanation of the potentiodynamic technique should be prefaced by a general description of corrosion processes--in particular, corrosion processes which occur in aerated and deaerated acidic aqueous solutions, since these are representative of the aniline hydrochloride system. Corrosion of metals proceeds by the following reaction with hydrogen ions in the solution:

$$2\,M + 2\,H^{+} \longrightarrow 2\,M^{+} + H_2$$

Electrons are transferred from the metal directly to the hydrogen ion via the metallic phase. The site of metal ion expulsion is the anodic site and the site of hydrogen evolution is the cathodic site. The anode refers to the site at which net oxidation occurs,and the cathode is the site at which net reduction occurs. These sites on the metal surface may be separated by a few atom diameters producing uniform corrosion or by greater distances causing non-uniform corrosion.[11] In addition to reaction with hydrogen ions, dissolved oxygen can enhance corrosion in acidic solutions as shown by the following reaction.

$$4\,M + O_2 + 4\,H^{+} \longrightarrow 4\,M^{+} + 2\,H_2O$$

A representation of the two oxidation-reduction processes can be seen in Figure 3.[11]

Obviously, a combination of the two processes will cause more corrosion than either one occurring independently. The net reactions of iron corroding in an acid aqueous solution in the presence of oxygen can be described by the following reactions.

Oxidation of Iron	$Fe \longrightarrow Fe^{2+} + 2e^-$
Reduction of Hydrogen Ions	$2H^+ + 2e^- \longrightarrow H_2$
Net Reaction	$Fe + 2H^+ \longrightarrow Fe^{2+} + H_2$
Oxidation of Iron	$Fe \longrightarrow Fe^{2+} + 2e^-$
Reduction of Oxygen	$\frac{1}{2}O_2 + 2H^+ + 2e^- \longrightarrow H_2O$
Net Reaction	$Fe + \frac{1}{2}O_2 + 2H^+ \longrightarrow Fe^{2+} + H_2O$

Both reactions occur simultaneously on the surface of the metal. The Gibbs free energy change for the reactions proceeding in the illustrated direction is negative at all values of pH.[11] Thus, iron corrodes in an acidic aqueous environment.

The rate at which these reactions proceed is dependent on several variables.

1. The concentrations of reactants and products in the solution.
2. The diffusion rate of species to and from the metal surface.
3. The presence of complexing agents in the solution which may stabilize metal ions.
4. The relative size and positions of local cathodes and anodes.

5. The formation of a protective barrier on the metal surface.
6. The temperature of the system.

The effect of most of these variables on the aniline hydrochloride system will be addressed in the Results and Discussion section.

Around 1890, at the Royal Institute, M. Faraday laid the groundwork for electrochemistry by formulating the following laws.(12)

1. The amount of chemical decomposition produced by a current is proportional to the quantity of electricity passed.
2. The amounts of different substances deposited or dissolved by a given quantity of electricity are proportional to their chemical equivalent weights.

Furthermore, Faraday determined the amount of electricity corresponding to one mole of electrons. This amount, called the Faraday constant, is equal to 96,487 coulombs per mole. These results allow calculation of metal dissolution rates in an electrochemical cell with a known amount of current flowing through it.

Faraday also found that half-cell potentials of an electrochemical cell deviated from their equilibrium potentials when current was allowed to flow through the cell.(11) An example of this effect is illustrated in Figure 4. When the two cells are electrically isolated from each other, each electrode assumes its equilibrium potential. If the two cells are shorted by means of a conductor, current flows from the zinc electrode to the platinum electrode,

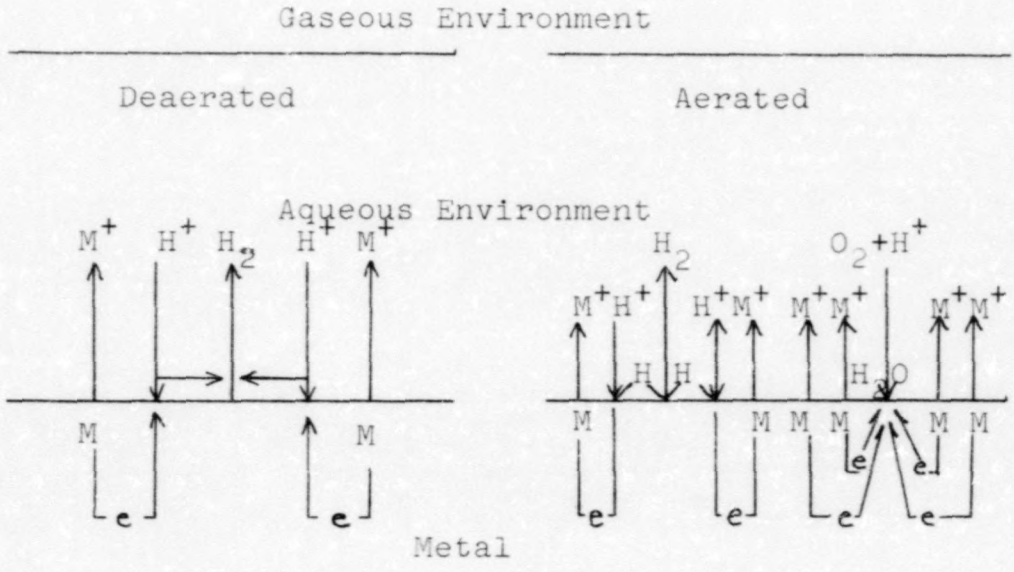

Figure 3. Oxidation-reduction reactions of a metal immersed in aerated and deaerated aqueous environments.

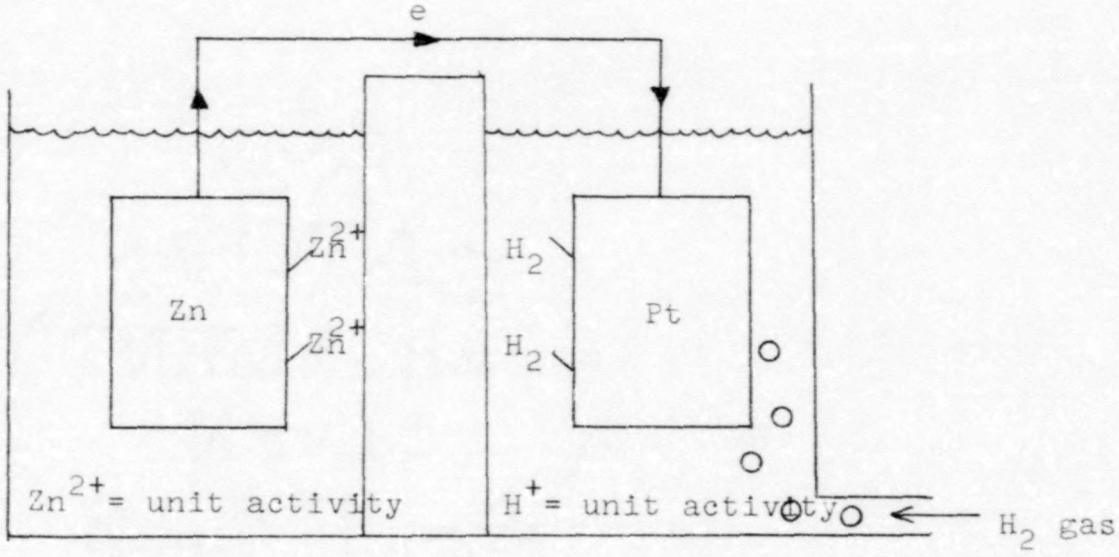

Figure 4. Electrochemical cell.

polarizing each to values other than their equilibrium potentials. Thus, polarization is the displacement of electrode potential resulting from a net current. The degree of polarization is measured in terms of overvoltage, frequently abbreviated as η, and is the displacement of potential relative to the equilibrium potential of the isolated half-cell.

Electrochemical polarization is composed mainly of two types: activation polarization and concentration polarization.[13] Activation polarization occurs when the electrochemical reaction is controlled by a slow step in the reaction sequence,and concentration polarization occurs when the reaction is controlled by diffusion of reacting species to the metal. In 1904, J. Tafel[14] proposed an equation which described overvoltage as a function of applied current for electrochemical reactions exhibiting activation polarization. Tafel found that the activation polarization for various electrode reactions could be expressed in the form $\eta = A + B\log i$, where A and B are constants and i is the current in amps.

Subsequent work by Stearn and Geary[15] determined the form of the Tafel equation to be $\eta = \pm\beta \log \frac{i}{i_o}$, where β is the Tafel constant, i is the current, and i_o is the exchange current density. This equation can be written as $\eta = -\beta \log i + \beta \log i_o$ representing cathodic polarization and $\eta = \beta \log i - \beta \log i_o$ representing anodic polarization. It can be seen that the preceding equations are of the form $y = mx + b$;and,thus, a plot of overvoltage (η) versus log i

will yield a straight line with slope β. In actual practice, the overvoltage curve is nonlinear within ±60 mV of the equilibrium potential but becomes linear at higher polarization voltages in a region called the Tafel region. The Tafel constant, β, represents the expression 2.3 RT/αnF, where n is the number of electrons transferred in the reaction, R is the gas constant, T is temperature in °K, F is the Faraday constant, and α is a symmetry coefficient defining the shape of the energy activation barrier. Extrapolation of the Tafel region for both anodic and cathodic polarization curves to the equilibrium potential defines the current at which oxidation and reduction reactions are equal. This current represents the equilibrium exchange current density.

According to the mixed potential theory developed by Wagner and Traud[16] in 1938, any electrochemical reaction can be divided into two or more partial oxidation and reduction reactions. Furthermore, there can be no net accumulation of charge during an electrochemical reaction. The mixed potential theory can best be described by the case of a mixed electrode system, where a metal is in contact with two or more oxidation-reduction reactions.

The case of iron corroding in an acidic solution is illustrated in Figure 5. The two half-cells, H_2/H^+ and Fe/Fe^{2+}, each exhibit an equilibrium potential and exchange current density as indicated in the Figure by E_{H/H^+}, $i_{o_{H/H^+}}$ and $E_{Fe/Fe^{2+}}$, $i_{o_{Fe/Fe^{2+}}}$. When the two cells are shorted, as when iron is immersed in an acidic solution, the potential of the iron stabilizes at a point between the

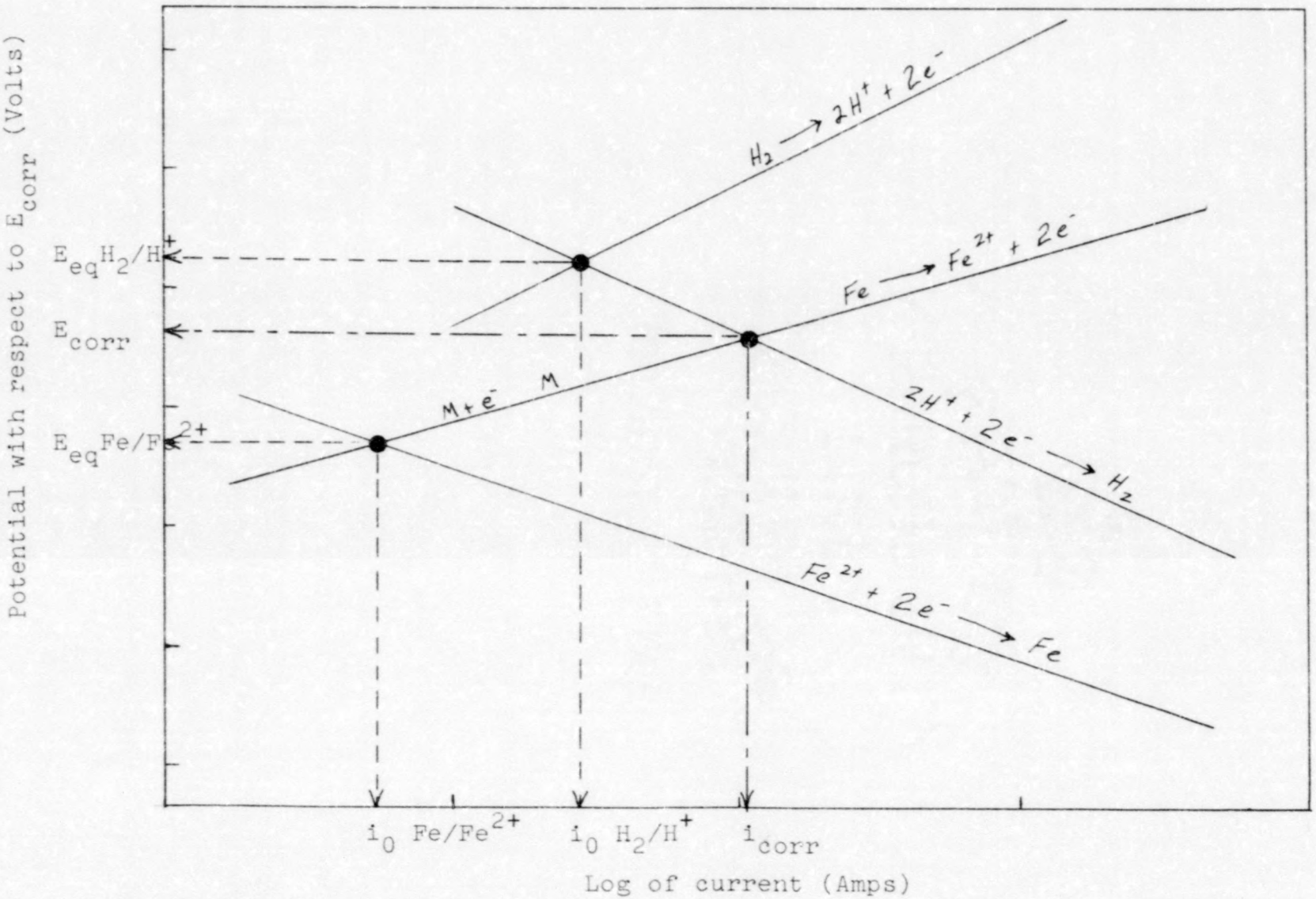

Figure 5. Potentiodynamic diagram for Iron exposed to an acidic solution.

two half-cell equilibrium ptentials. This potential is called the corrosion potential and is usually represented by E_{corr}. The point at which oxidation and reduction reactions are equal defines the corrosion current, I_{corr}, thus satisfying the second postulate of the mixed potential theory which states that there can be no net accumulation of charge during an electrochemical reaction.

A polarization experiment of iron immersed in an acidic solution would reveal only the iron dissolution and hydrogen evolution reactions. Extrapolation of the Tafel regions in both anodic and cathodic polarization curves to the corrosion potential defines the corrosion current from which a corrosion rate in mils per year can be calculated. The Figure represents an oversimplification of most systems. Any number of oxidation-reduction reactions can occur depending on the system, which can complicate the interpretation of the data.(17)

Tafel extrapolation is the basis for potentiodynamic corrosion rate determinations. A schematic for the instrumentation used when making potentiodynamic corrosion measurements is shown in Figure 6. The metal sample or specimen is termed the working electrode,and currents are supplied to it by means of one or more platinum auxillary electrodes. Platinum is used since it is relatively inert. The potential of the working electrode is measured with respect to a reference electrode enclosed in a Luggin capillary probe. The Luggin probe reduces the resistance between the reference and working electrodes. In the case of cathodic polarization,

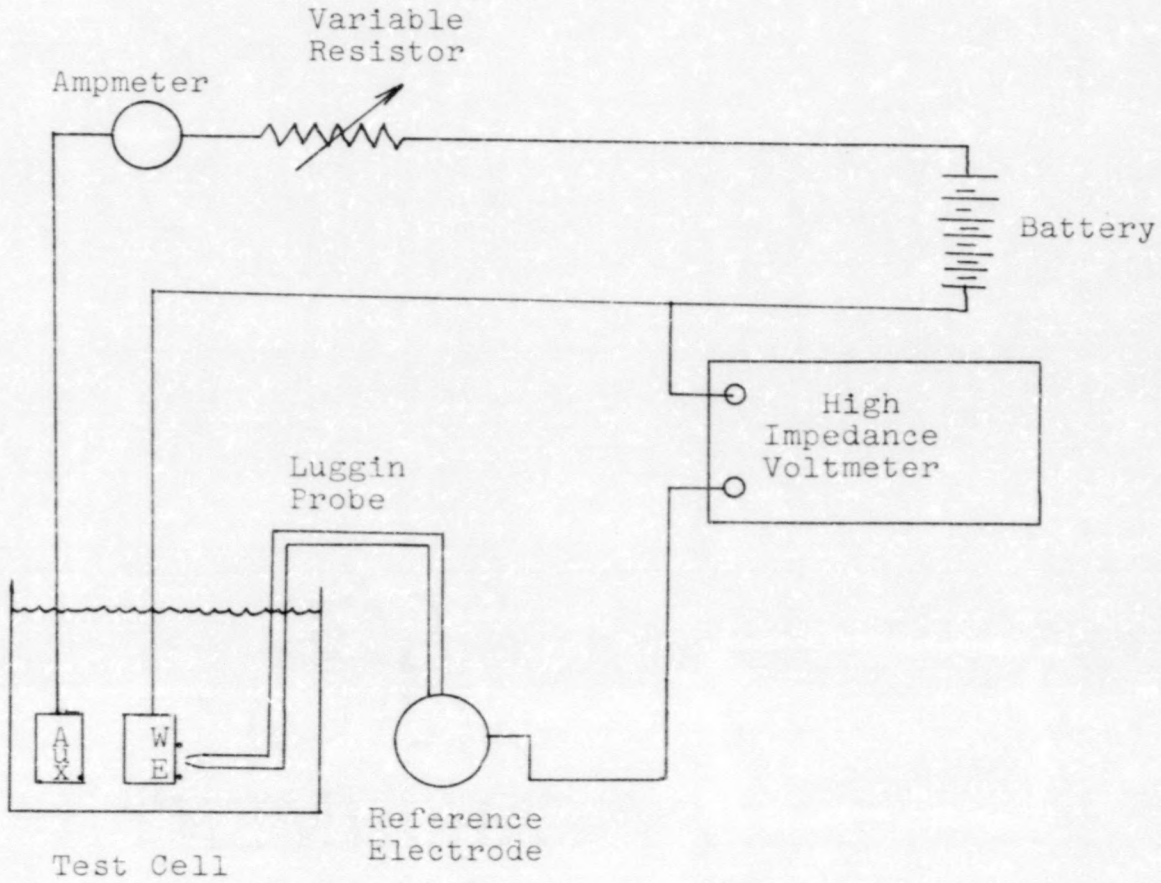

Figure 6. Instrumentation schematic for potentiodynamic corrosion rate measurements.

the potential of the working electrode is decreased incrementally by means of an externally applied current. Both the potential of the working electrode and the current required to maintain that potential at each increment is measured. In anodic polarization, the potential of the working electrode is increased with respect to the equilibrium potential. The resulting curve from anodic and cathodic polarization is shown in Figure 7. The curves are nonlinear in the region ±60 mV from the equilibrium potential, but become linear in the Tafel region. Extrapolation of the Tafel regions to the equilibrium potential defines the equilibrium exchange current density.

It is not uncommon to observe deviation from linearity at the high currents, particularly in the cathodic polarization curves.[17] This deviation is shown in the Figure and is due to concentration polarization. Concentration polarization is often exhibited by the cathodic reaction where, during high reaction rates, as in the case of a high applied current density, the concentration of the reacting species is depleted near the surface of the metal.[17] The current at which the reaction becomes concentration limited is termed the limiting diffusion current and is defined by the equation, $i_L = \frac{DnFC_B}{\sigma}$, where D is the diffusion coefficient of the reacting species in the solution, n is the number of electrons transferred, C_B is the bulk solution concentration of the species, F is the Faraday constant, and σ is the thickness of the double layer of ions on the surface of the polarized electrode. In the case of an electrode

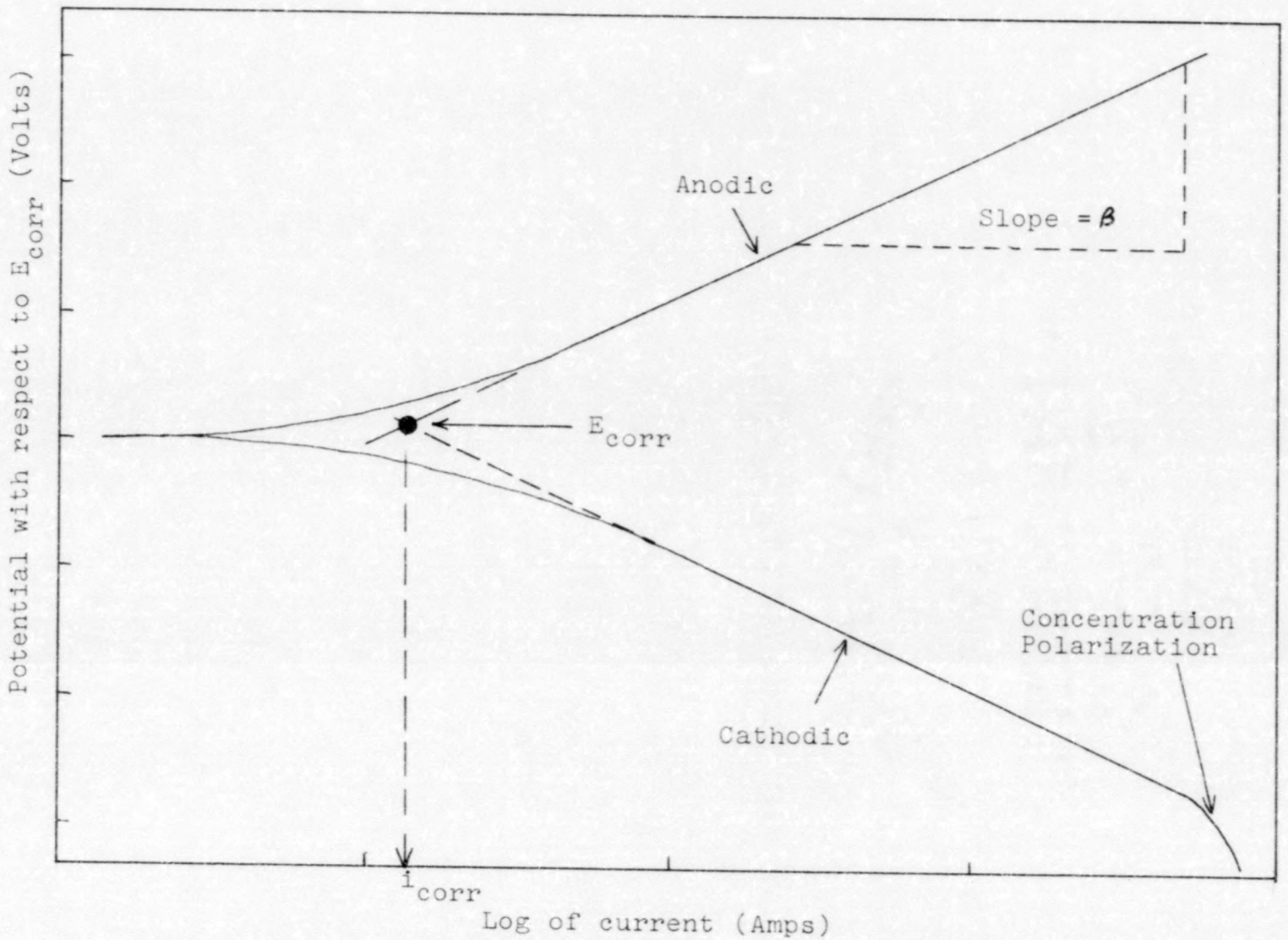

Figure 7. Example of anodic and cathodic polarization curves from potentiodynamic corrosion rate measurements.

exhibiting only concentration polarization, the relationship between overvoltage and the limiting current is represented by $\eta_c = 2.3 \frac{RT}{nF} \log(1 - \frac{i}{i_L})$. The anodic reaction is very rarely diffusion limited and, therefore, the overvoltage expression as a function of current is the same as for activation polarization, $\eta = \beta \log i\frac{i}{i_o}$.(11) There exists a linear relationship between concentration of the reacting species near the metal surface and the diffusion limiting current. Increasing the bulk concentration of reacting species will increase the diffusion limiting current.

An example of concentration polarization in the cathodic reduction of hydrogen can be seen in Figure 8. As the current approaches the limiting current the polarization becomes very large. Increasing bulk concentrations or increasing solution velocity will cause the limiting current to shift to higher values. In many cases, what one sees in the cathodic polarization curve is a combination of both activation and concentration polarization, which can make interpretation of the data much more difficult. In the case of the combined processes, the equation for dependence of overvoltage on the current would be

$$\eta = -\beta \log \frac{i}{i_o} + 2.3 \frac{RT}{nF} \log(1 - \frac{i}{i_L} \quad (11)$$

activation polarization — concentration polarization

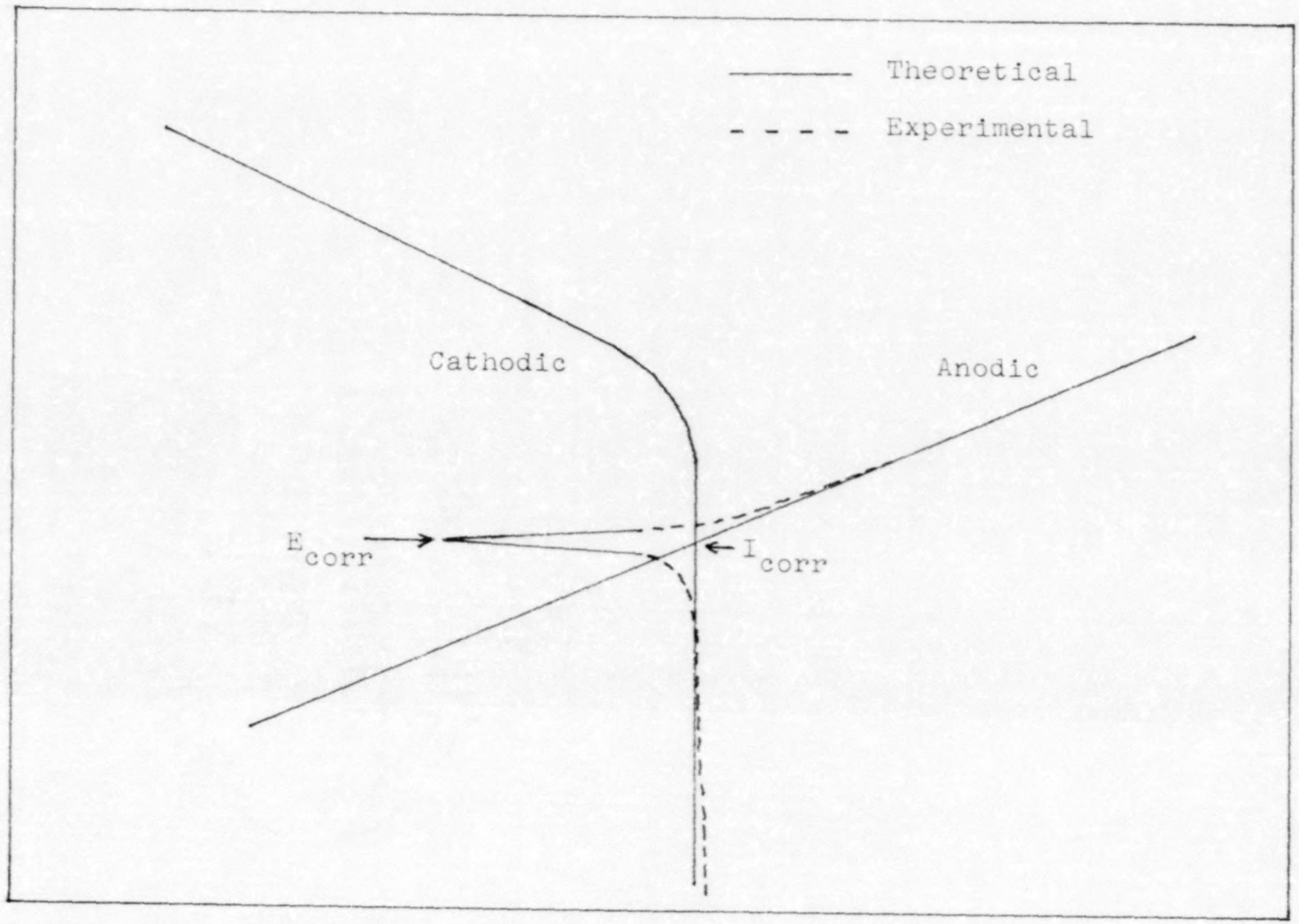

Figure 8. Illustration of concentration polarization.

Corrosion Inhibitors

An additional aspect of the aniline hydrochloride system under investigation is the inhibiting effect of aniline. An inhibitor is a compound, which, when added to the environment in small concentrations, decreases or prevents corrosion of a metal. Inhibitors may act as passivators, precipitators, neutralizers or adsorbants. Their function in protection of the metal may be by:[18]

1. formation of layers of considerable thickness.
2. formation of films by reaction with the metal.
3. surface adsorption without reaction with the metal.

Organic inhibitors such as aniline are typically adsorption inhibitors.[18] The compound may adsorb by means of pi-bond adsorption, chemisorption, electrostatic adsorption, or any combination of the three. There is evidence in the case of aniline in acidic media that the anilinium ion found in solution is attracted to metal surfaces where it loses a proton and is adsorbed as a neutral compound, thus forming a protective film of the free amine.[19] The aniline does not change the overall reaction but does decrease corrosion rates by forming a barrier to diffusion of the reacting species in the solution to the metal surface. Thus, in a potentiodynamic experiment, the corrosion current i_{corr} would shift to lower values after the addition of the inhibitor.

It has been determined that aniline and its derivatives are all cathodic as well as anodic inhibitors.[18] That is, they form protective films on cathodic and anodic sites on the metal surface. The adsorption of organic films can lead

to some interesting observations in potentiodynamic experiments, as will be discussed later in this thesis.

A computer literature review conducted through the last decade failed to reveal any information on aniline hydrochloride corrosion. A limited amount of information of a semiquantitative nature is available from the corrosion data survey.[20]

EXPERIMENTAL TECHNIQUE

Due to the preliminary nature of this work, many different experiments were performed which deviated from any one set experimental technique. These experiments were designed to determine optimum conditions,and the following text details those conditions which were found to be the most appropriate. Deviations from the described technique will be noted were appropriate.

Potentiodynamic Corrosion Technique

Instrumentation

An Electrochemoscope IIB computerized corrosion monitoring system developed by ECO Instruments, a subsidiary of SeaData Corporation, was used in the potentiodynamic work. The system can be considered "state-of-the-art" technology and is one of the best systems commercially available.

The system consists of an ECO Instruments model 553/EPU digital potentiostat/galvanostat with voltage and current outputs of ±50 V and ±1 Amp,respectively. The potentiostat was interfaced via a RS232 interface to a Hewlett-Packard HP-86 computer which was equipped with two HP9130A disc drives, an HP7470A graphic plotter and an Epson MX80111 dot matrix printer. The test cell was an ASTM glass cell with two platinum counter electrodes, a saturated Calomel

reference electrode enclosed in a Luggin Probe, a teflon specimen holder and a gas bubbler. (See Figure 9 for detailed design of the test cell.) The software for the system was provided by ECO Instruments and included programs for linear polarization, cyclic polarization, and several others, as well as the potentiodynamic program which was used for this work. Figure 10 illustrates data flow for the system.

The potentiostat is controlled and monitored by the computer which can access programs and store or retrieve data from the disc drives. During a scan the data is temporarily stored in the computer and permanently stored on a disc after a scan. This data can then be retrieved and processed by the computer and printed out in hard copy by the printer and plotter.

Specimen preparation

A flat sheet of carbon steel M1044 with an approximate thickness of 4 mm was cut square and turned on a lathe to a flat circular specimen with a diameter of 11.34 mm. See Table 1 for composition of M1044 steel.[21] A steel sheet metal screw was soldered to one face of the specimen. The assembly was then cold-mounted in epoxy resin with the screw protruding through the resin and the opposite face of the specimen exposed. The similar composition of the specimen and the screw would prevent a galvanic coupling effect between the two.

The specimen was prepared by grinding the exposed face with 400 then 600 grit silicon carbide paper, washing with

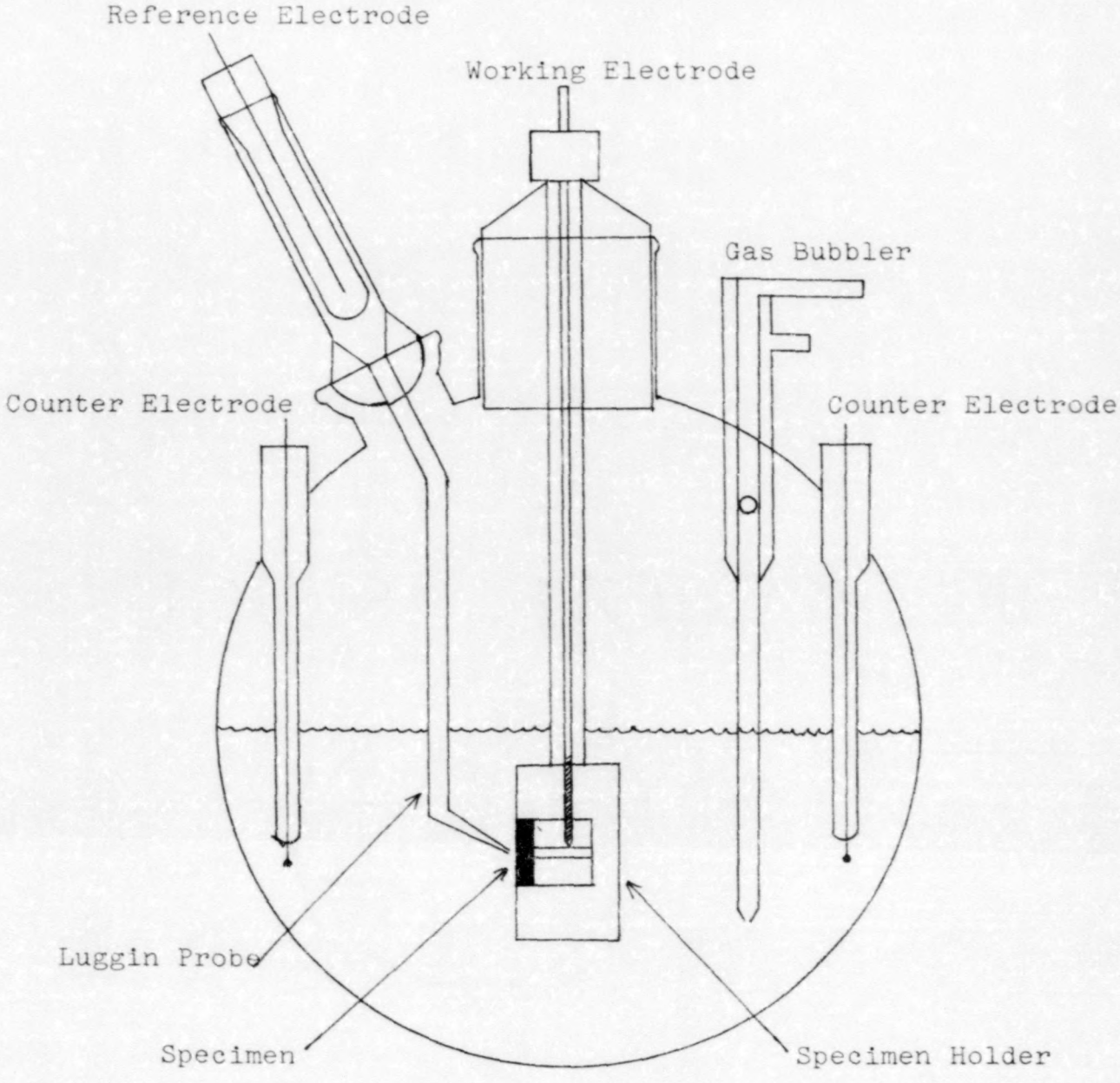

Figure 9. Electrochemical test cell.

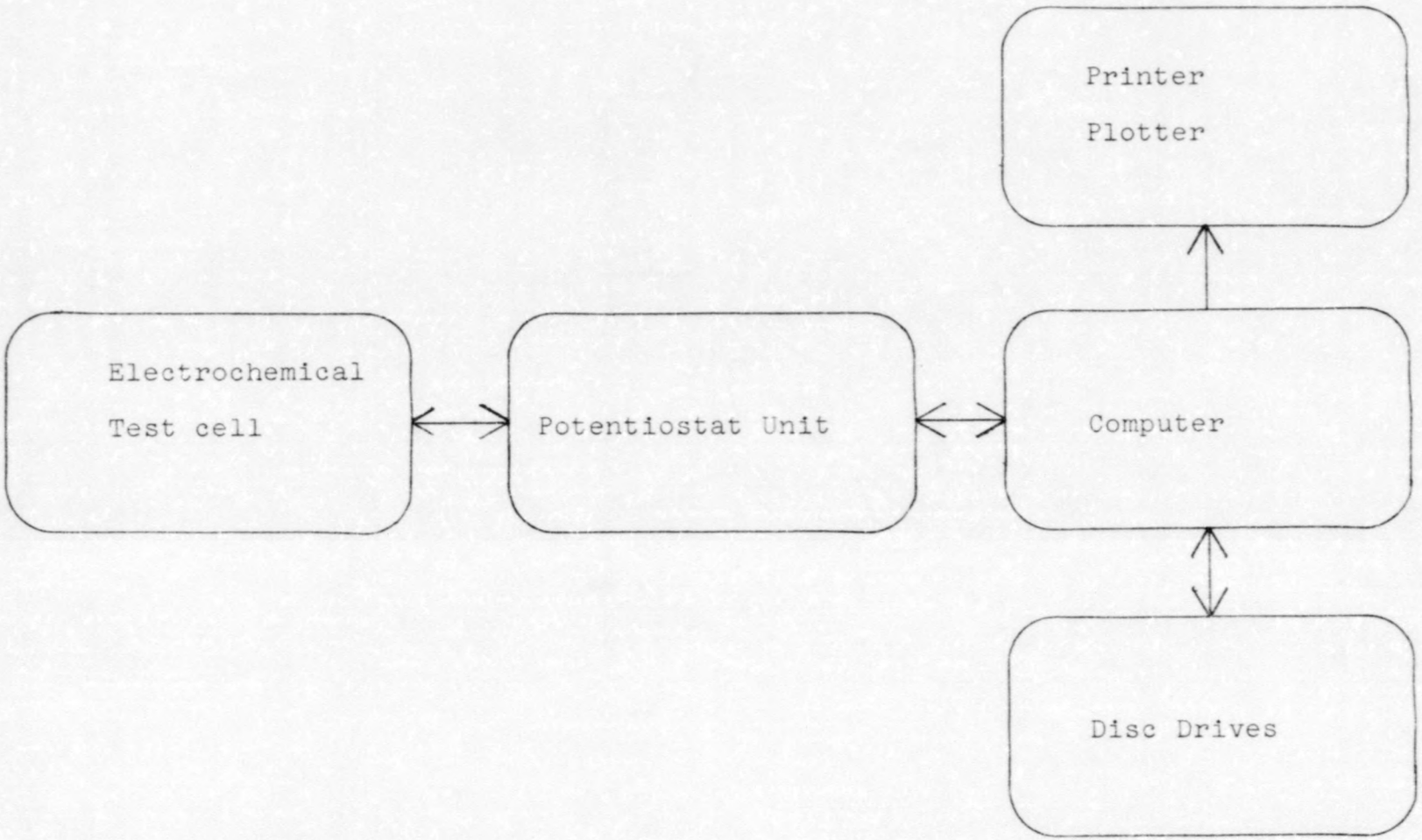

Figure 10. Flow diagram for computer controlled potentiodynamic corrosion testing system.

Table 1. Composition of Carbon Steel M 1044.

% Carbon	% Manganese	% Phosphorus	% Sulfur
0.43-0.50	0.60-0.90	0.04 max	0.50 max

Balance - Iron

deionized distilled water (DD water), and swabbing with methanol. The specimen was immediately placed in the teflon holder, and continuity between it and the external connection was verified prior to immersion into the test solution. The same specimen was used for successive experiments and was prepared by this procedure each time prior to the experiment.

Solution preparation

Solutions were prepared on a weight-to-weight basis from reagent grade aniline hydrochloride and DD water. An insoluble impurity, probably produced by oxidation of aniline, had to be removed from the solutions by filtration prior to use. All solutions were used within 3 to 4 days after preparation. In some experiments solid aniline hydrochloride was added directly to the cell; in this case the impurity was present during the experiment. It was not clear whether or not the impurity affected the results since particles of the impurity had a tendency to collect on the surface of the specimen.

For air-free experiments the solutions were prepared by two methods:

1. In situ deaeration by bubbling ultra high purity nitrogen through the solution overnight while agitating.

2. Bubbling nitrogen through boiling DD water before preparing a solution which was filtered directly into the cell. It is probable that both methods were approximately as effective in removing oxygen. Later experiments[22] showed that the concentration of oxygen in the solution after several hours of bubbling was less than 0.05 ppm, the lower threshold of the oxygen detector. Actual concentrations may be lower. Nitrogen was bubbled continuously through the solution in the cell during the air-free experiments. In aerated experiments, where the solution was exposed to the atmosphere, oxygen concentration was found to be about 10 ppm.[22]

Resistance measurements

Solution resistance measurements were made using an AC signal generator to impose an AC current between the working and reference electrodes and an oscilloscope to measure the phase change between the two input signals from the reference electrode and the generator. A high impedance voltage follower was used on the reference output to compensate for high resistance solutions.

Prior to a measurement, stirring was stopped and the system allowed to equilibrate for about two minutes. This was found to be necessary since noise, due to the stirrer and solution agitation, prevented accurate measurements.

A schematic of the diagram is shown in Figure 11. After all components were powered, both channels of the oscilloscope were zeroed before a measurement was made. The AC signal on channel 1 was then adjusted so that the maximum

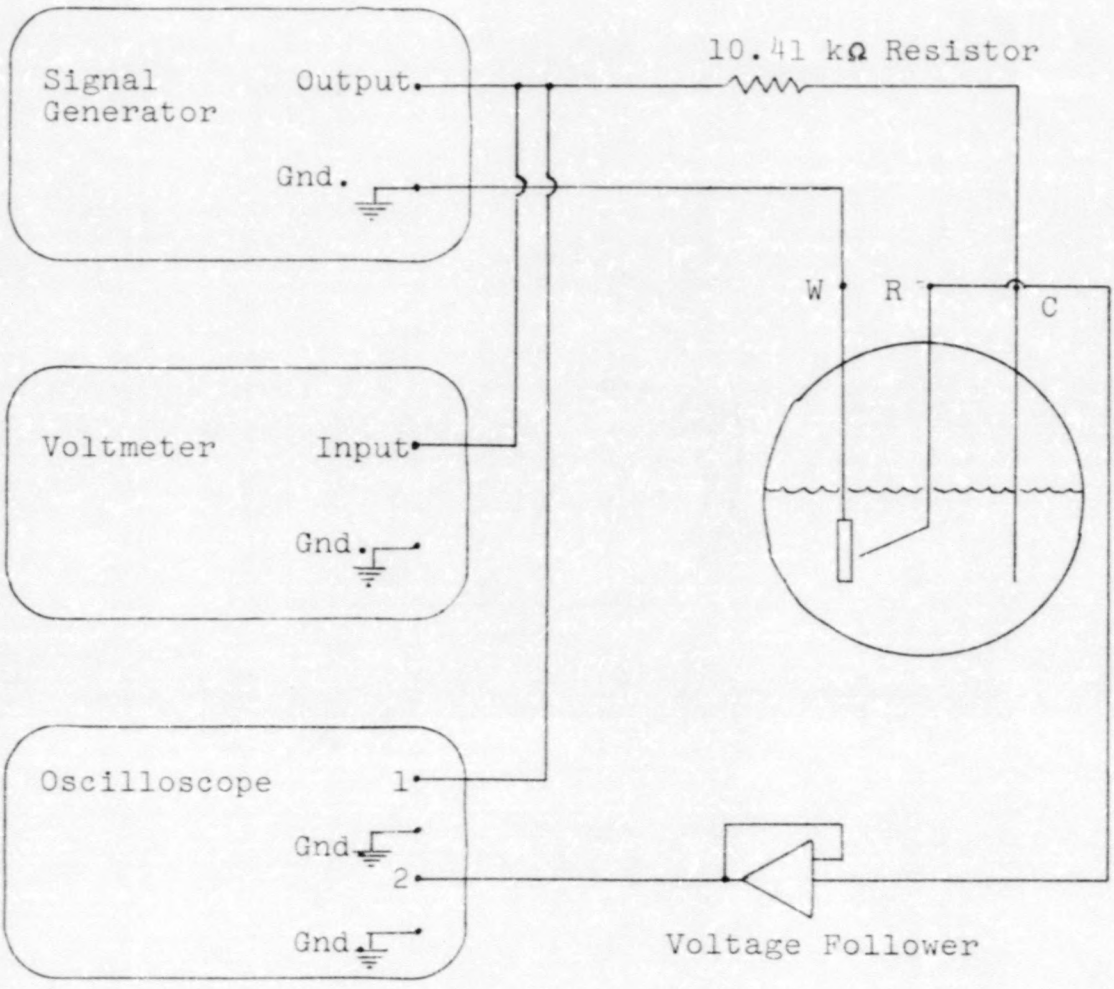

Figure 11. Wiring diagram for resistance measurements.

was in the center of the scope scale. The reference electrode signal on channel 2 was slightly out of phase with the generator signal. (See Figure 12 for details.) The in-phase component of the reference electrode signal is proportional to the resistance.[23] We assumed that the current through the cell is in phase with the generator's voltage since the cell impedance was usually much lower than 10 kΩ. As the frequency was adjusted from low values (100 Hz) to high values (20 kHz) the reference electrode signal would begin high in amplitude, decrease to a minimum over a certain range, and then increase again as a result of stray capacitances. A frequency in the middle of the minimum range was chosen since it best represents the effects of the inter-electrode resistance.[23] Erroneous results were obtained if frequencies very far above or below this range were used. This frequency was found to be 1 kHz for high concentration solutions (ca. 1000 ppm) and about 10 kHz for low concentrations (ca. 100 ppm).

The effective voltage (V_{eff}) of the AC signal from the generator was set at about 7 volts and the in-phase component of the reference signal (V_f) was measured on the oscilloscope. Solution resistance was then calculated as follows:

$$\frac{V_f}{V_{eff} \times \sqrt{2}/10410\Omega} = \text{Solution Resistance } (\Omega)$$

It is assumed that the resistance is due to the liquid only and does not change during the course of an experiment. This assumption may be invalid at high anodic current densities

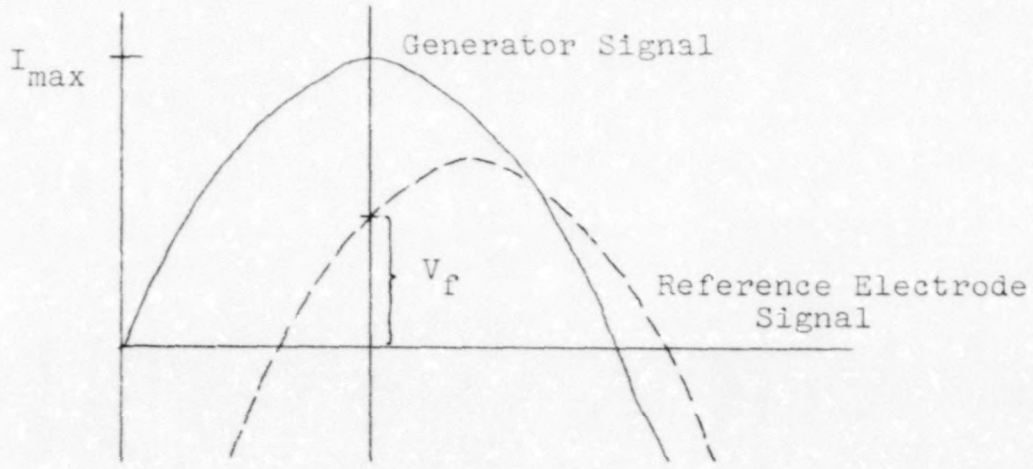

Figure 12. Phase shift due to solution resistance.

as changes in the surface of the specimen may alter the interelectrode resistance.

Typical solution resistance was in the order of two to three ohms. Accuracy of the V_f measurement was about ±0.5 mV and therefore resistance was measured to within about ±0.5Ω. Resistance measurements were made at appropriate intervals during an experimental series.

Potentiodynamic scans

Approximately 500 ml of test solution was placed in the electrochemical cell. The solution was agitated with a magnetic stirrer, and all scans except those taken in static solutions were agitated at about the same rate. Exact velocities are not known. All scans were made at room temperature (23 ± 1°C). The specimen was inserted into the teflon holder and placed in the solution at time t_0. The solution and specimen were allowed to equilibrate for 20 minutes to 2 hours prior to running a scan. The potentiodynamic

program instructed the potentiostat to increase or decrease voltage, depending on whether the scan was anodic or cathodic, between the counter and working electrodes in 10 mV increments at a rate of 130 μV/sec. The computer reported the average of several sampled values taken at each 10 mV increment. After the scan had reached the upper voltage level the system was allowed to return to its open electrode potential (E_{corr}) and the data processed and displayed. The data were plotted and, after the solution resistance was entered into the computer, another plot using the corrected voltages was drawn thus giving both solution resistance corrected and uncorrected curves for comparison. The corrected voltages were calculated as follows:

$$E_{corrected} = E_{uncorrected} - R \times I$$

R = Solution Resistance

I = Current

A series of scans could be run for a single solution in this manner. The linear or Tafel region of the corrected curve, if observed, was extrapolated to E_{corr} giving the corrosion current I_{corr}. Corrosion rate in mils per year (MPY) was then calculated with the following equation:

$$\frac{I_{corr}(A)}{A \times 2.177} = MPY;$$ where,

A = Coupon Area (cm^2)

2.177 is a conversion constant converting A/cm^2 to MPY, assuming pure iron and $Fe \longrightarrow Fe^{2+} + 2e^-$

Weight Loss Measurements

Coupon preparation

Rectangular specimens of carbon steel M1044, obtained from the same lot as the electrochemical specimen, were polished with 400, then 600, grit silicon carbide paper, then washed with DD water and finally swabbed with methanol. For area calculations, coupon dimensions were measured to within ±0.1 mm. Coupon area was calculated as follows:

$$2(LW) + 2(LT) + 2(WT) + 2\pi(RT) - 2\pi R^2 = \text{Area}$$

L = Length W = Width T = Thickness R = Hole radius

A hole was drilled in the coupon so that the specimen could be suspended in the test solution. Coupons were used the same day of preparation. The same coupons were used repeatedly after repreparation.

Experimental technique and conditions

Approximately 500 ml of test solution, prepared the same as potentiodynamic solutions, were placed in standard weight loss jars (1 quart mason jars) equipped with glass hangers for suspending the test coupons. The liquid was in constant contact with the air. Exact volumes of test solution were not determined. The solutions were either static during the weight loss measurements or agitated with magnetic stirrers at two rates of agitation: slowly stirred and fast stirred. Exact stirring velocities are not known. Experiments were performed at room temperature (23 ± 1°C). Coupons were weighed to the nearest 0.1 mg before placing them in the test solution at time t^0 and removing them at time t. The coupons were rinsed with DD water, washed with methanol, and placed

in an ultrasonic methanol bath until further sonication removed no more corrosion products. Coupons were then reweighed and the weight loss calculated. Duplicate coupons were used in each flask and the average weight loss reported. The corrosion rate in MPY was calculated as follows.

$$\frac{\text{Weight Loss (mg)}}{\text{Coupon Area (cm}^2\text{) x Time (t-t}_0\text{)}} \times (6.3 \times 10^{-7}) = \text{MPY}$$

The number 6.3×10^{-7} is a conversion factor converting mg/cm^2sec to MPY assuming pure iron and $Fe \longrightarrow Fe^{2+} + 2e^-$.

RESULTS AND DISCUSSION

Corrosion rates of carbon steel M1044 were determined in aqueous solutions of aniline hydrochloride, varying in concentration from 0.0028 M to 0.1410 M, by the potentiodynamic and weight loss corrosion measuring techniques at various rates of agitation and oxygen concentrations.

Weight Loss Corrosion Measurements

Plots of corrosion rate versus coupon exposure time for the weight loss measurements had a tendency to fluctuate markedly in the first few hours before leveling out to a fairly linear region. A typical example of this effect can be seen in Figure 13 where corrosion rate is plotted versus average time of immersion for carbon steel M1044 in an agitated aqueous solution containing 500 ppm chloride as aniline hydrochloride. Average time means that the point is placed on the x axis at the middle of the time interval. This procedure is common in weight loss measurements since the total corrosion over a time interval is measured rather than rates at each time. Corrosion rates obtained from weight loss data are not very accurate and may deviate ±50 MPY from the average rate.

The average corrosion rates after the first five hours of carbon steel M1044 immersion in aerated solutions of various concentrations of aniline hydrochloride at three

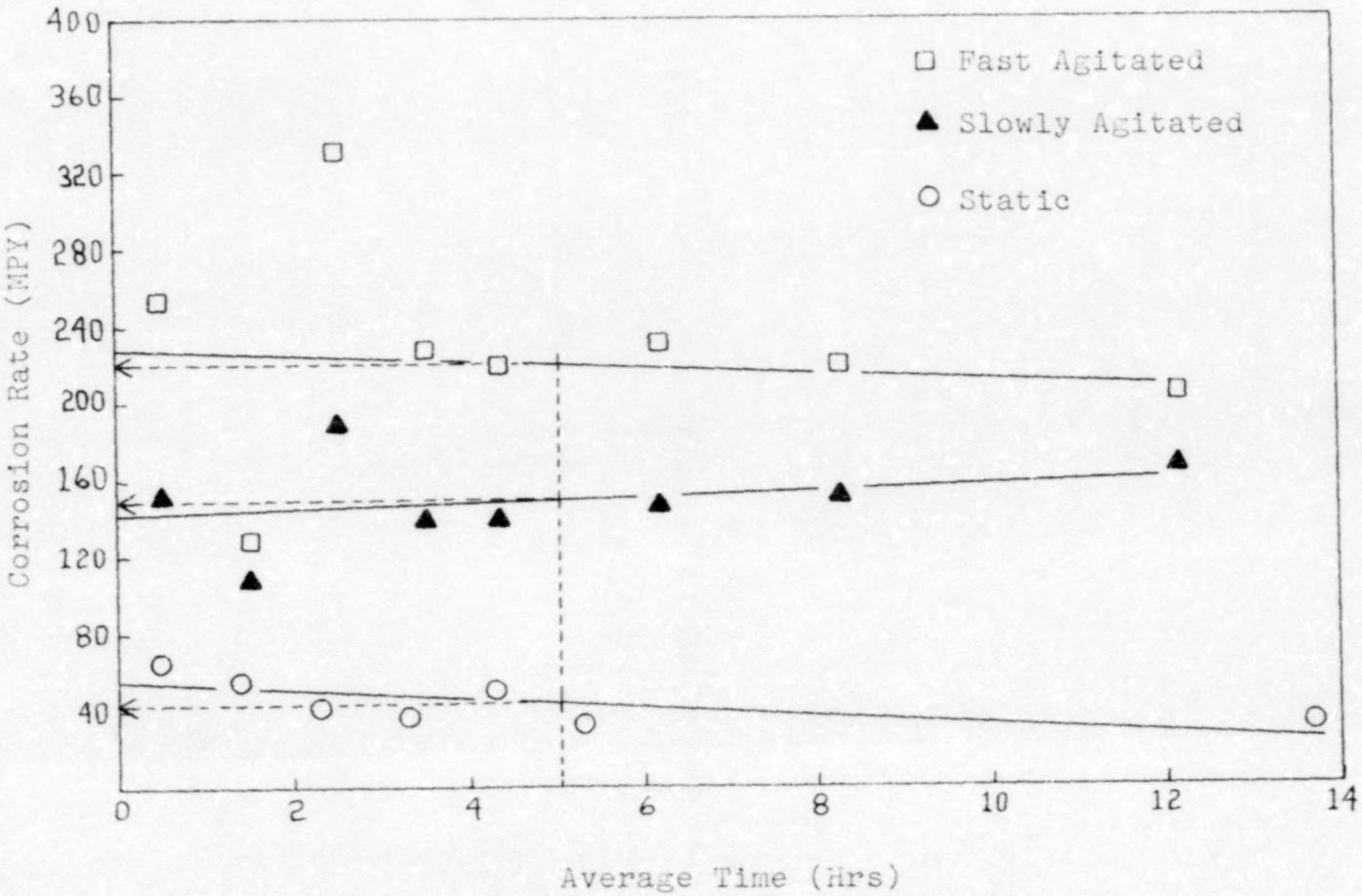

Figure 13. Weight loss corrosion rate versus time for a 500ppm chloride aerated aqueous solution.

rates of agitation are listed in Table 2. Concentration is expressed as ppm chloride. Figure 14 is a graphical representation of this data. It is clear from the graph that corrosion is dependent on the rate of agitation. Static solutions give the lowest rates and fast agitated solutions give the highest. The slowly agitated solutions are intermediate. This effect is observed in corrosion systems when corrosion is limited by the rate of diffusion of a reacting species in the solution to the surface of the metal.[11] By increasing solution velocity an increase in transport occurs and correspondingly an increase in corrosion rate. The reacting species can be termed a limiting diffusion species.

In many corrosion systems open to the atmosphere, the rate of corrosion is dependent on the concentration of oxygen in the system. In these systems oxygen acts as a limiting diffusion species. Increasing the concentration of oxygen in the bulk solution or increasing diffusion of oxygen to the metal surface will result in higher corrosion rates. The evidence suggests that corrosion in the aerated aniline hydrochloride system could be oxygen diffusion limited.

Weight loss measurements in deaerated 1000 ppm chloride solutions show a significantly lower corrosion rate compared to aerated solutions of the same concentration and agitation rate. The data are listed in Table 3. The average corrosion rate after five hours in aerated 1000 ppm solution is about 200 MPY as compared to about 50 MPY in the deaerated solution. This result indicates that oxygen is, in a large part, responsible for the corrosion and that lowering oxygen

Table 2. Weight loss corrosion rates versus concentration of aniline hydrochloride (aerated).

Concentration (ppm chloride)	Corrosion Rate (± 50 MPY) Static Solution	Agitated Slowly Solution	Agitated Fast Solution	pH
100	20	-[a]	-	3.65
200	35	210	-	3.52
400	45	190	-	3.35
500	45	150	220	3.27
1000	60	125	205	3.13
2000	30	110	185	2.96
4000	25	-	-	-

[a]Data not available.

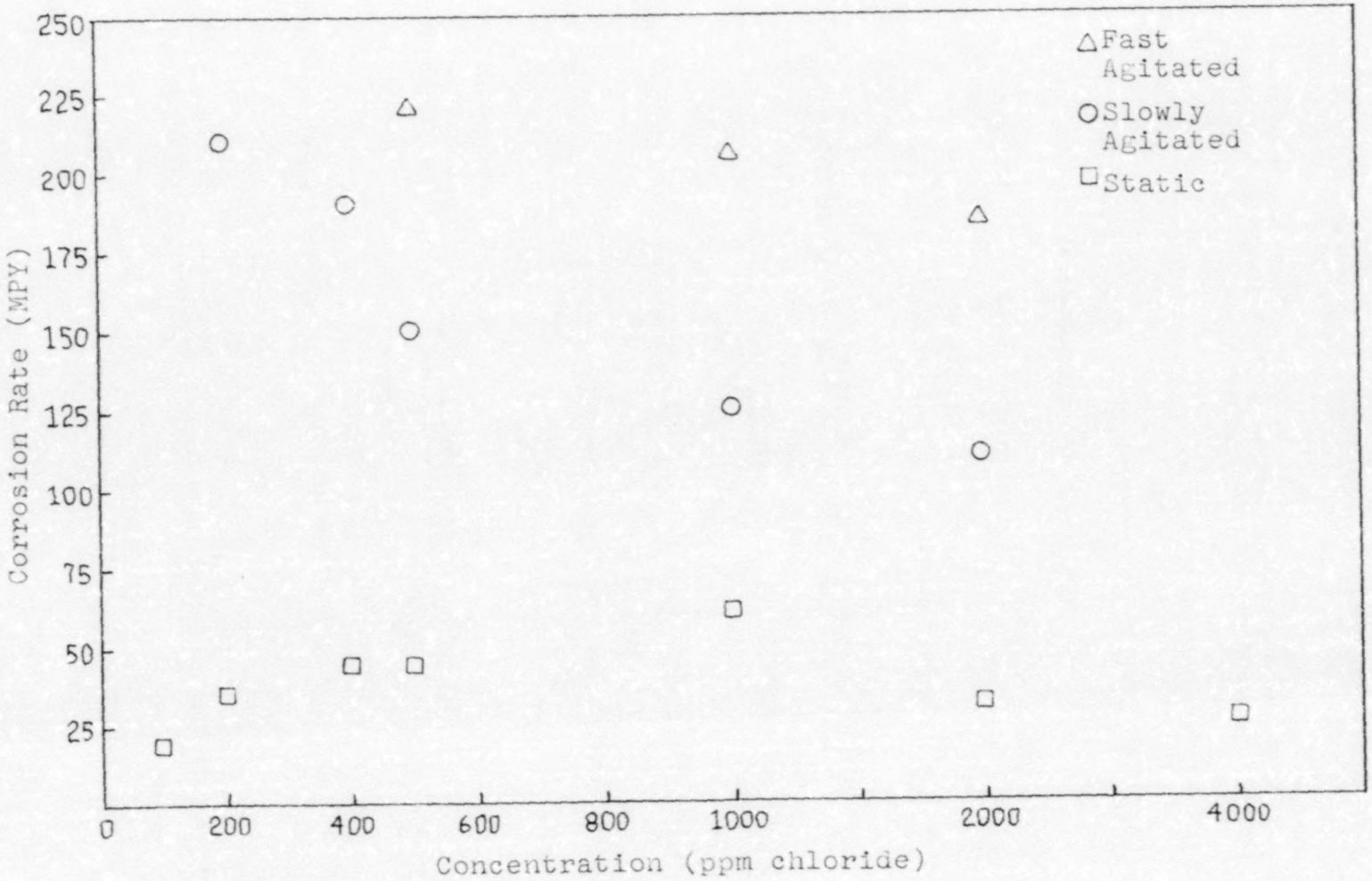

Figure 14. Weight loss corrosion rate versus concentration for aerated solutions.

Table 3. Corrosion rate in aerated and deaerated 1000 ppm aniline hydrochloride solutions.

Immersion Time (Hrs)	Corrosion rate (MPY) 1000 ppm aerated	Corrosion rate (MPY) 1000 ppm deaerated
2.0	198 ± 50	52 ± 50
5.5	235 ± 50	52 ± 50

concentrations can significantly reduce corrosion. This behavior is typical of oxygen diffusion limited systems.

In aerated acid corrosion systems the typical corrosion reactions involve both hydrogen ions and molecular oxygen. In the case of iron corroding in an aqueous acidic environment in the presence of oxygen, the following overall reaction would occur.[11]

$$Fe + \tfrac{1}{2}O_2 + 2H^+ \longrightarrow Fe^{2+} + H_2O$$

The dependence of corrosion rate on pH for the aniline hydrochloride system is shown in Figure 15. It can be seen from the graph that corrosion rate generally decreases with decreasing pH except for the initial increase found in the static solutions. The static solutions do show a decrease at the lower pH range. Since all measurements were taken under the same conditions, one would expect the oxygen concentration in all the solutions to be approximately the same. Although oxygen solubility in water does decrease with increasing chloride concentration, this effect is probably negligible in the range measured in this work. Assuming oxygen concentration to be the same in all solutions, the decrease in corrosion rate with increasing hydrogen ion

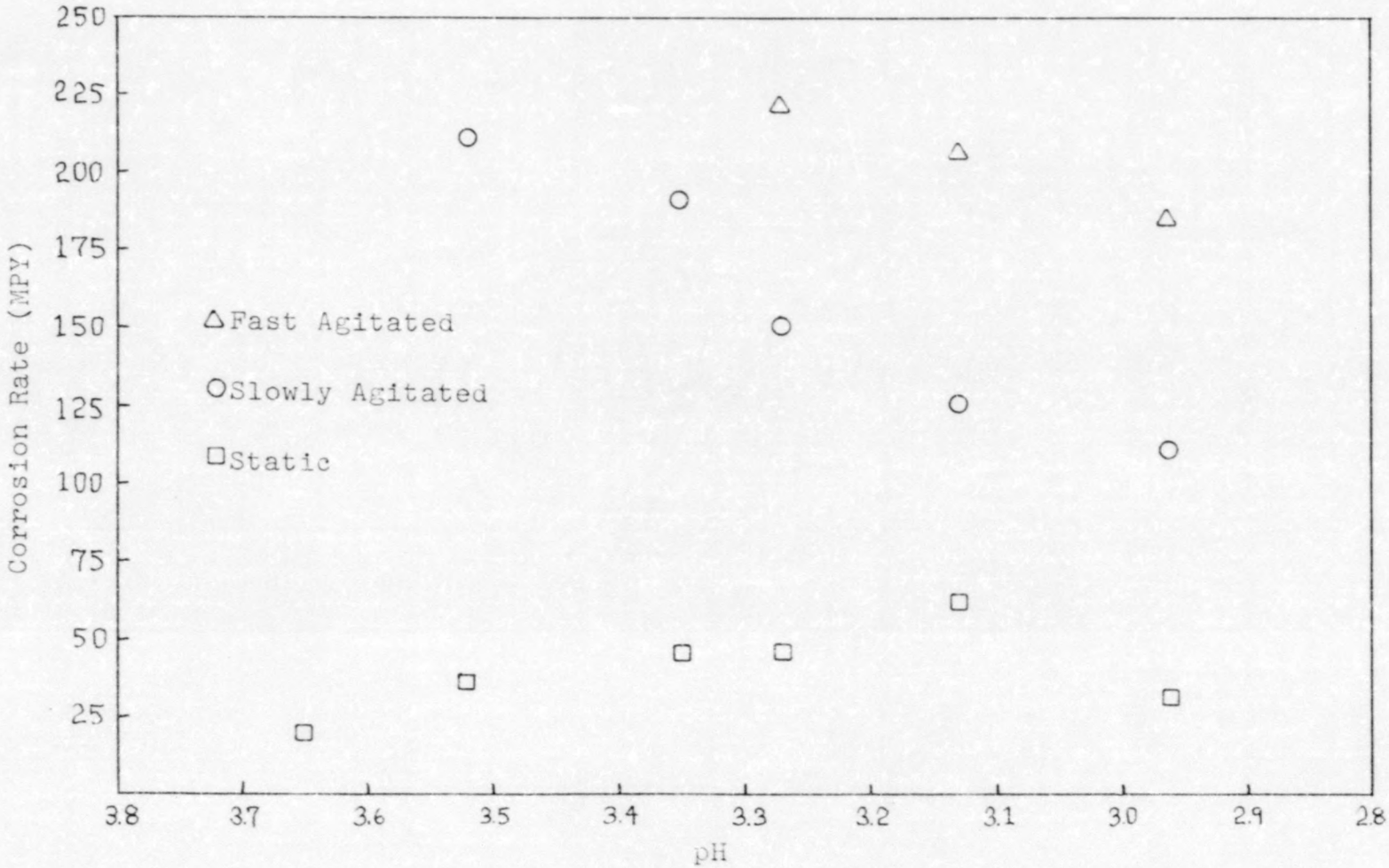

Figure 15. Weight loss corrosion rate versus pH for aerated solutions.

concentration (decreasing pH) suggests the formation of a surface film which inhibits diffusion of reacting species to the surface of the metal. Other evidence presented in this thesis supports this theory.

A passive layer or film could be formed by adsorption of aniline or anilinium ions attracted to cathodic sites on the metal surface. The mechanism of ion adsorption followed by deprotonation and subsequent adsorption of the free base has been proposed elsewhere.[19] As more molecules are adsorbed, a film forms on the surface of the metal thereby preventing oxygen and hydrogen ions from reaching the surface and reacting. Conversely, expulsion of Fe^{2+} ions from anodic sites on the metal would be hampered as well. The largest decrease in corrosion, however, would be due to the decrease in oxygen concentration at the metal solution interface.

The initial increase in corrosion rate with increasing concentration observed in the static solutions does not agree with the idea of film formation unless the diffusion of anilinium ions to the surface of the metal is considered. Since it is very difficult to obtain a true static solution, due to convection created by thermal effects and by hydrogen evolution at the metal surface, it is conceivable that in static solutions at low concentrations of aniline hydrochloride the anilinium ion concentration would not be sufficient to overcome convection effects and form a protective film. Thus, a critical concentration may be required for effective film formation. This critical concentration appears to be reached at about 1000 ppm aniline hydrochloride for the static solutions

corresponding to an anilinium ion concentration of about 0.0235 M. Above 1000 ppm aniline hycrochloride a surface film is formed--or more likely, it becomes effective enough so that corrosion rates decrease as the hydrogen ion concentration increases. Bulk solution agitation may increase the effective concentration of anilinium ions at the metal solution interface and allow film formation at lower bulk concentrations than static solutions. This effect was observed in the agitated solutions.

It was useful, for comparison purposes, to determine corrosion rates of carbon steel M1044 in aqueous solutions of acetic acid and potssium chloride to that of equivalent concentrations of aniline hydrochloride. Acetic acid was chosen since it has a similar dissociation constant to that of anilinium ion, 1.76×10^{-5} as compared to 2.34×10^{-5}, and would therefore produce a similar hydrogen ion concentration and buffering effect. The average corrosion rate after five hours in an agitated 0.0282 M acetic acid solution was 205 MPY as compared to 190 MPY for an equimolar solution of aniline hydrochloride, whereas an agitated 1000 ppm solution of potassium chloride gave a 35 MPY five hour average.

Solutions in Contact with Air

Potentiodynamic measurements were taken in solutions identical to those for wieght loss measurements in order to gain further insight into the mechanism of corrosion and the chemistry of the system.

Potentiodynamic versus weight loss corrosion rates taken at equivalent time intervals in 0.0282 M acetic acid

and 1000 ppm potassium chloride are listed in Table 4. Correlation between the two techniques is shown in Figure 16. A least squares fit of the data is described by the equation $y = 0.939\ x - 7.75$, where y is the weight loss corrosion rate and x is the electrochemical corrosion rate. The correlation coefficient for the data is 0.959. A slope of one and a y intercept of zero would describe a perfect fit. A correlation coefficient of one is a perfect correlation.

According to the Stearn and Geary treatment of Tafel extrapolation, described in the introduction section of this thesis, extrapolation of the Tafel regions of anodic and cathodic overvoltage versus log of current curves should intersect at the open circuit potential (E_{corr}) and define the corrosion current (I_{corr}), from which the corrosion rate can be calculated. The aniline hydrochloride system did not demonstrate this behavior as the two curves generally did not intersect at E_{corr} but were displaced a certain amount on the current coordinate thus defining anodic and cathodic corrosion currents Ia_{corr} and Ic_{corr}, respectively. The first 60 mV of the curves were ignored and the next 200 mV extrapolated back to the corrosion potential. It was found that the amount of displacement appeared to be a linear function of the pH as will be shown later. Due to the disagreement between cathodic and anodic values for I_{corr} the two will be described separately before they are discussed jointly.

In almost all cases the cathodic values of I_{corr} correlated better with weight loss measurements than did anodic values. A

Table 4. Potentiodynamic versus weight loss corrosion rates for aerated solutions of 0.0282 M acetic acid and 1000 ppm potassium chloride.

0.0282 M Acetic Acid

Immersion Time (Hrs)	Potentiodynamic Corrosion rate (MPY)	Weight Loss Corrosion rate (MPY)
5.6	213	205
5.9	189	205
7.6	244	190
1000 ppm Potassium Chloride		
2.2	63	35
3.0	64	35
7.3	27	35

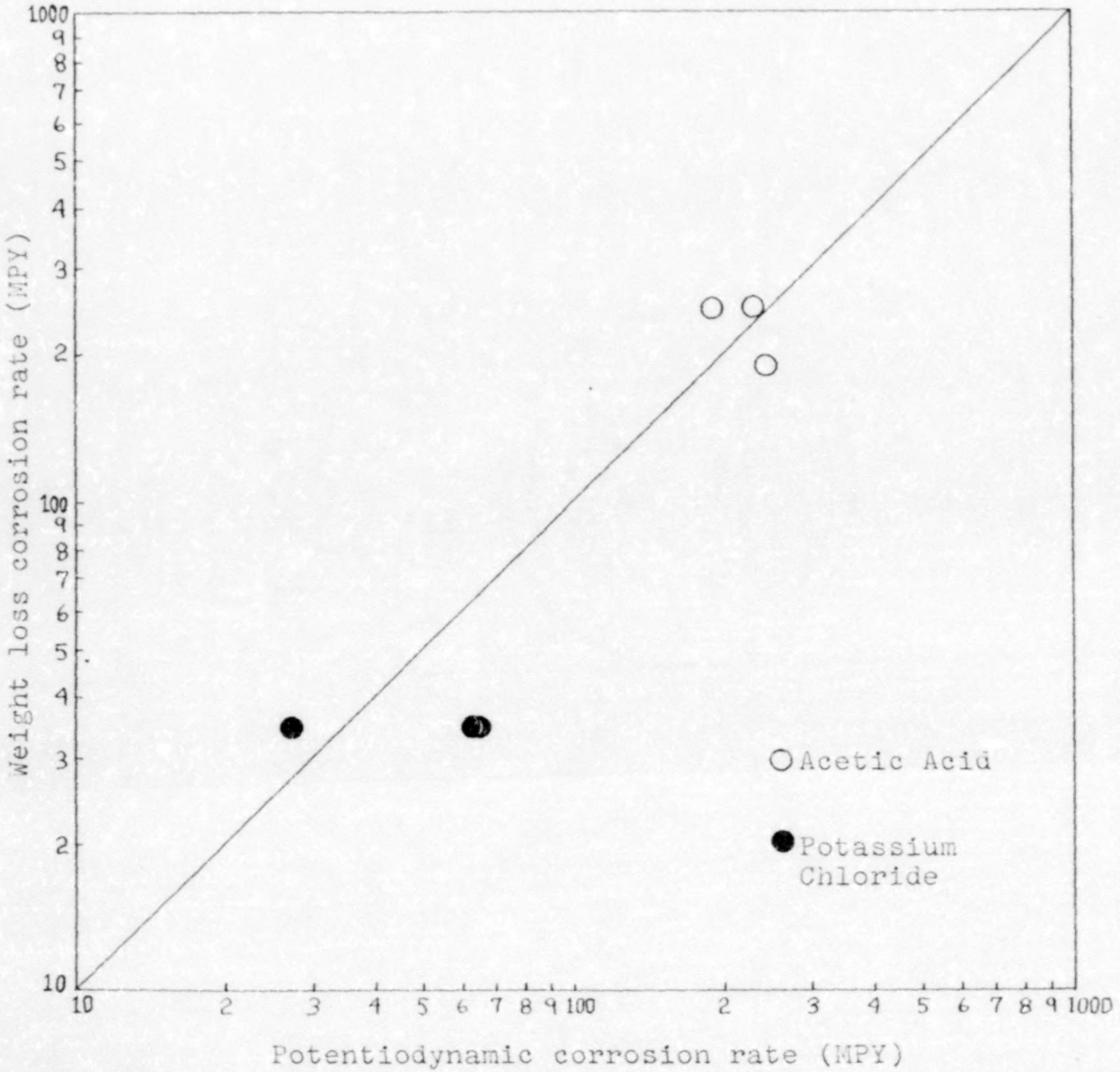

Figure 16. Potentiodynamic versus weight loss corrosion rate for aerated 0.0282 M acetic acid and 1000ppm potassium chloride.

comprehensive list of potentiodynamic versus weight loss corrosion rates for agitated 1000 and 2000 ppm aniline hydrochloride solutions is shown in Table 5. Data are listed for deaerated 1000 ppm solutions, illustrating the lower corrosion rate of the air-free system and providing points for the low end of the corrosion rate range. Figure 17 is a graphical representation of the data. Although there is a definite correlation between the data generated by the two methods in the aniline hydrochloride system, correlation is not as good as that observed with acetic acid and potassium chloride. It should be noted that the heaviest concentration of points appears to the right of the ideal correlation line, thus indicating that the potentiodynamic measurements were generally higher than the weight loss measurements. This was true in almost all cases. The data from the potentiodynamic measurements in the carbon steel-aniline hydrochloride system are not easily interpreted.

A series of potentiodynamic experiments were performed in which corrosion rates were determined in various concentrations of aniline hydrochloride at static and agitated solution velocities. The data are listed in Table 6 along with pH values for the initial solutions. The pH of the solution does change with time as the specimen corrodes and hydrogen ions are depleted, however this change appears to be negligible over the time interval of the tests due to the large volume of the solution (500 ml) and to the buffering effect of anilinium ions. Furthermore, the concentration of Fe^{2+} ions

Table 5. Potentiodynamic versus weight loss corrosion rates for agitated solutions of aniline hydrochloride.

Immersion Time (Hrs)	Potentiodynamic Corrosion rate (MPY)	Weight Loss Corrosion rate (MPY)
1000 ppm aniline hydrochloride (aerated)		
0.6	238	281
1.0	353	185
1.1	300	185
1.4	208	185
2.0	387	165
3.8	134	198
4.3	213	198
5.8	169	235
1000 ppm aniline hydrochloride (deaerated)		
1.8	16	52
2.1	60	52
2.3	57	52
2.3	11	52
3.9	17	52
4.0	9	52
4.2	16	52
5.2	102	52
2000 ppm aniline hydrochloride (aerated)		
0.3	189	171
0.8	238	171
1.3	273	156
3.7	344	196
9.0	169	211
10.6	189	211
11.2	203	211

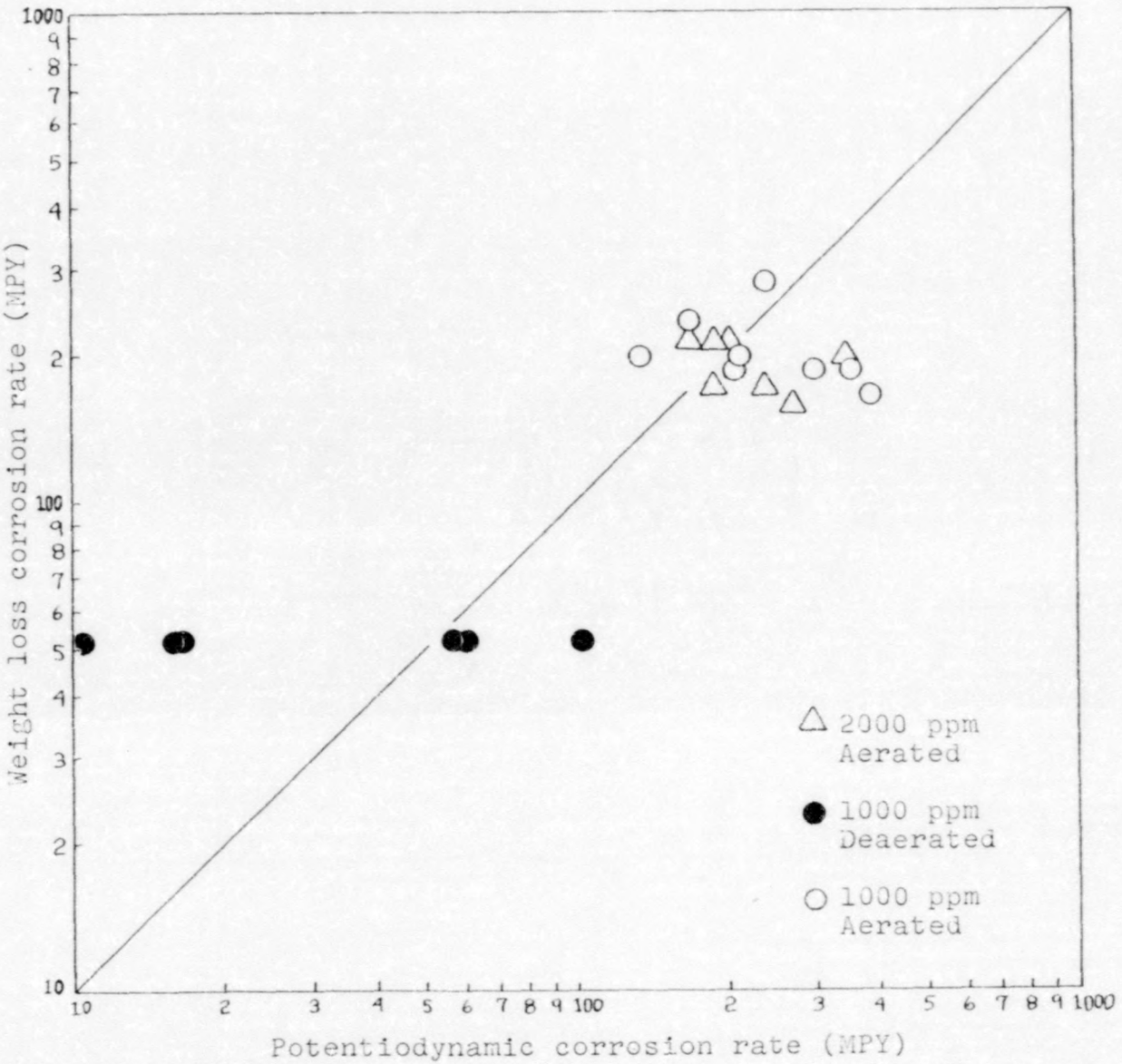

Figure 17. Potentiodynamic versus weight loss corrosion rate for solutions of 1000 and 2000 ppm aniline hydrochloride.

Table 6. Potentiodynamic data for aerated sclutions of aniline hydrochloride.

Concentration	Immersion Time (Hrs)	Solution Velocity	Cathodic/ Anodic	Ecorr	Log Icorr	MPY	pH
100	1.0	Agitated	Cat.	-649	-2.96	498	3.65
	1.3	Static	Cat.	-702	-4.06	40	
	2.1	Agitated	And.	-644	- [a]	-	
200	1.1	Static	Cat.	-686	-3.74	83	3.52
	2.5	Agitated	Cat.	-638	-2.88	599	
	2.8	Agitated	And.	-634	-3.43	169	
400	1.1	Static	Cat.	-681	-3.52	137	3.35
	1.8	Agitated	Cat.	-626	-2.77	772	
	2.0	Agitated	And.	-621	-3.10	361	
800	1.0	Agitated	Cat.	-611	-3.07	387	3.20
	1.3	Static	Cat.	-667	-3.33	213	
	1.4	Agitated	And.	-614	-2.85	642	
1000	1.1	Agitated	Cat.	-610	-3.18	300	3.13
	1.3	Static	Cat.	-664	-3.39	185	
	2.3	Agitated	And.	-604	-2.82	688	
2000	1.3	Agitated	Cat.	-593	-3.22	273	2.96
	1.8	Agitated	And.	-593	-2.51	1404	

[a] Data not available

does not appear to change significantly unless the specimen corrodes for more than a few hours or an anodic scan is run. Since no more tests were performed after an anodic scan, it is probable that the concentrations of components in the solution remained approximately constant over the time interval of the tests. The open circuit potentials (E_{corr}) were measured prior to running a scan and therefore reflect concentrations of components at that time.

Tracings of the anodic and cathodic overvoltage curves for this series are shown in Figures 18 and 19, respectively. The cathodic curves for static solutions of 100 to 800 ppm chloride and the agitated 100 ppm solution all show behavior characteristic of concentration polarization.[24] These curves define limiting diffusion currents for a reacting species in the solution. As the concentration of aniline hydrochloride increases, the slope of the curves become less steep suggesting a combination of activation and concentration polarization. In the agitated solutions activation polarization is oberved at lower concentrations than in the static solutions.

The relative positions of log I_{corr}, derived from cathodic curves, for the agitated and static solutions versus concentration of aniline hydrochloride expressed as ppm chloride is shown in Figure 20. Log I cathodic and thus corrosion rates in the static solutions increase up to 800 ppm then decrease, whereas the agitated corrosion rates begin to decrease at about 400 ppm. This observation is

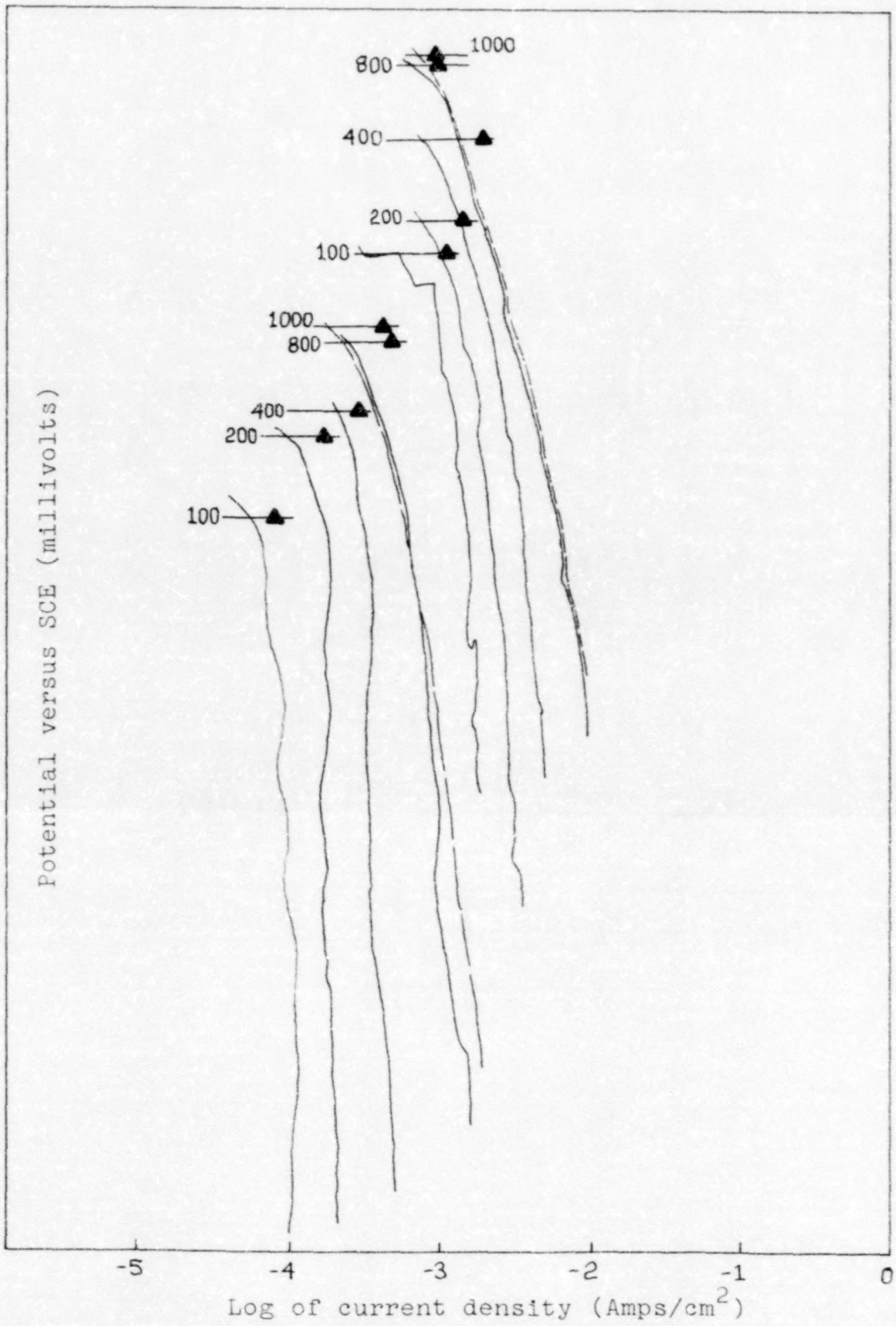

Figure 18. Cathodic potentiodynamic curves for aerated solutions.

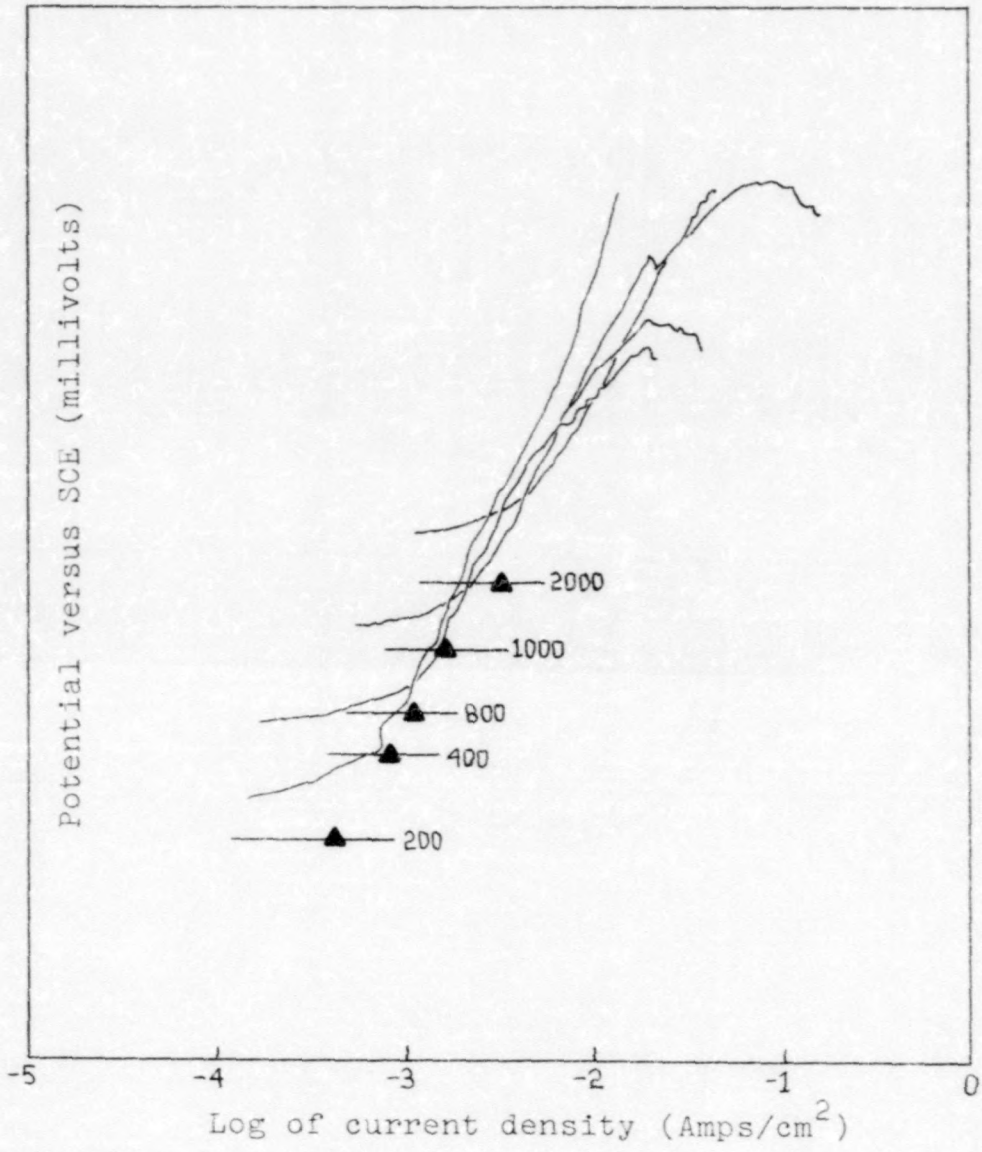

Figure 19. Anodic potentiodynamic curves for aerated solutions.

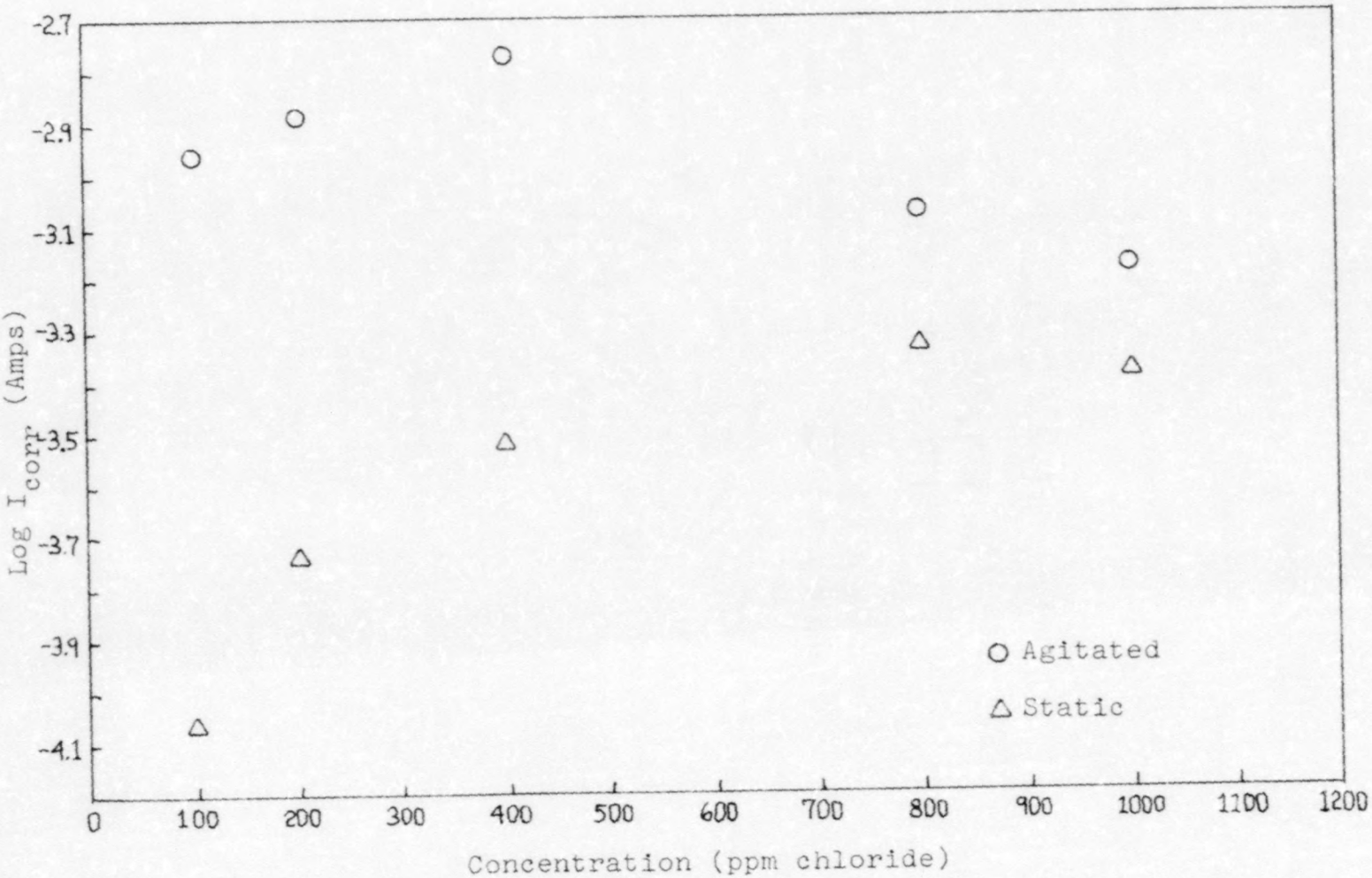

Figure 20. Log I_{corr} versus concentration for cathodic curves.

comparable to the weight loss experiments where it was noted that static solutions showed decreases in corrosion rates at higher concentrations than did agitated solutions. As the concentration of aniline hydrochloride increases,the difference between log I cathodic and thus corrosion rate for the two agitation rates becomes smaller. This suggests that the effect of the two agitation rates on the corrosion becomes more similar and that agitation produces a smaller effect as the concentration of aniline hydrochloride increases. The formation of a surface film could explain this effect since the film would act as a barrier to the diffusion of reacting species to the surface of the metal and would diminish velocity effects. Figure 21 shows that somewhat linear relationship between the difference in corrosion rate of the two agitation modes versus the concentration of aniline hydrochloride expressed as ppm chloride. This result supports the view that the surface film becomes more effective as the concentration increases.

There is a good linear correlation between potentiodynamically calculated and weight loss corrosion rates for the static solutions; however, the potentiodynamic rates are consistently higher than weight loss rates. This observation is illustrated in Figure 22. There is not sufficient data to determine a correlation between the two methods for the agitated systems.

The variation in corrosion potential with pH for all of the solutions listed in Table 6 is shown in Figure 23. Corrosion potential shows a definite linear relationship to

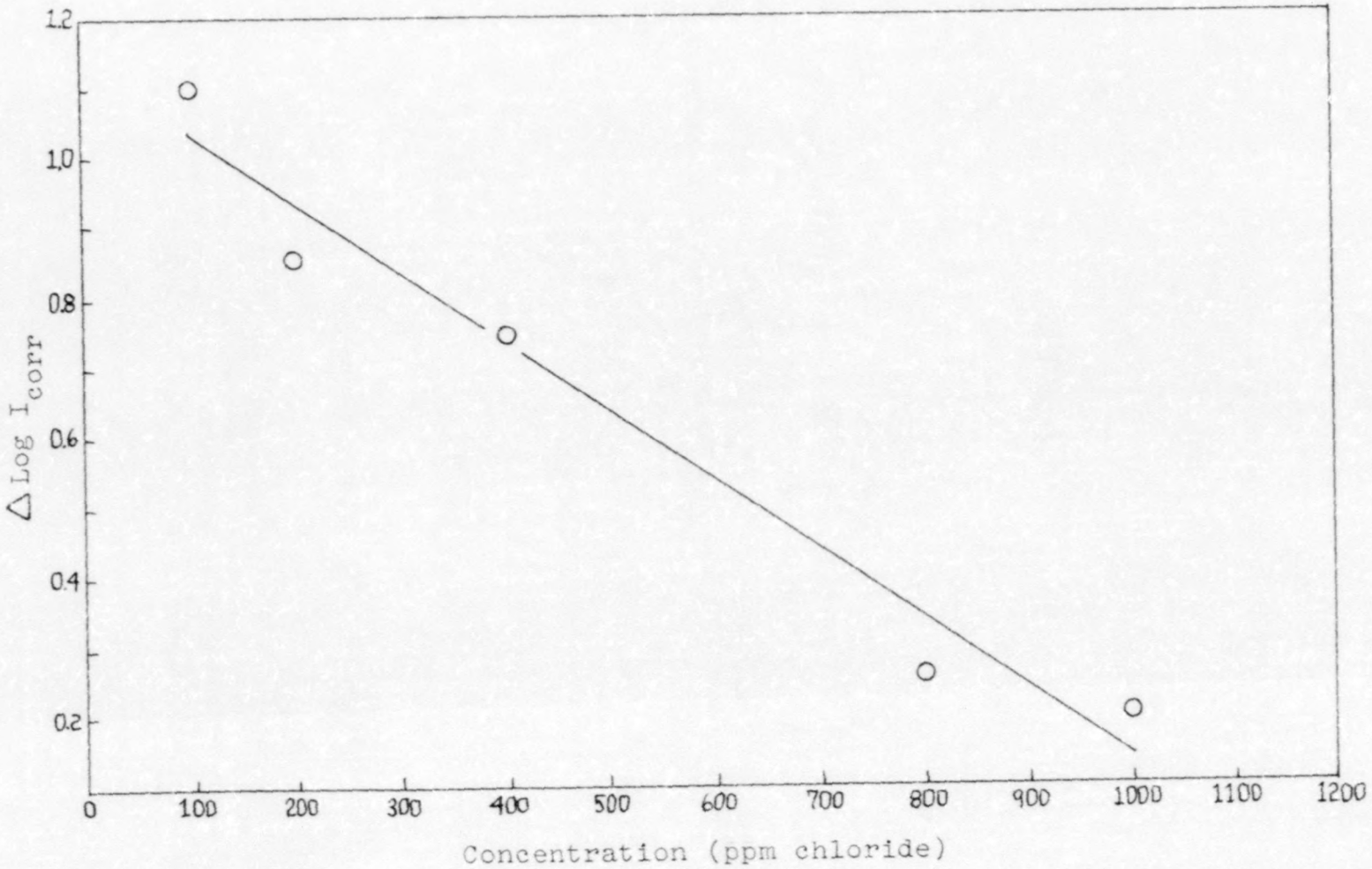

Figure 21. (Log I_{corr} agitated - Log I_{corr} static) versus concentration for cathodic curves.

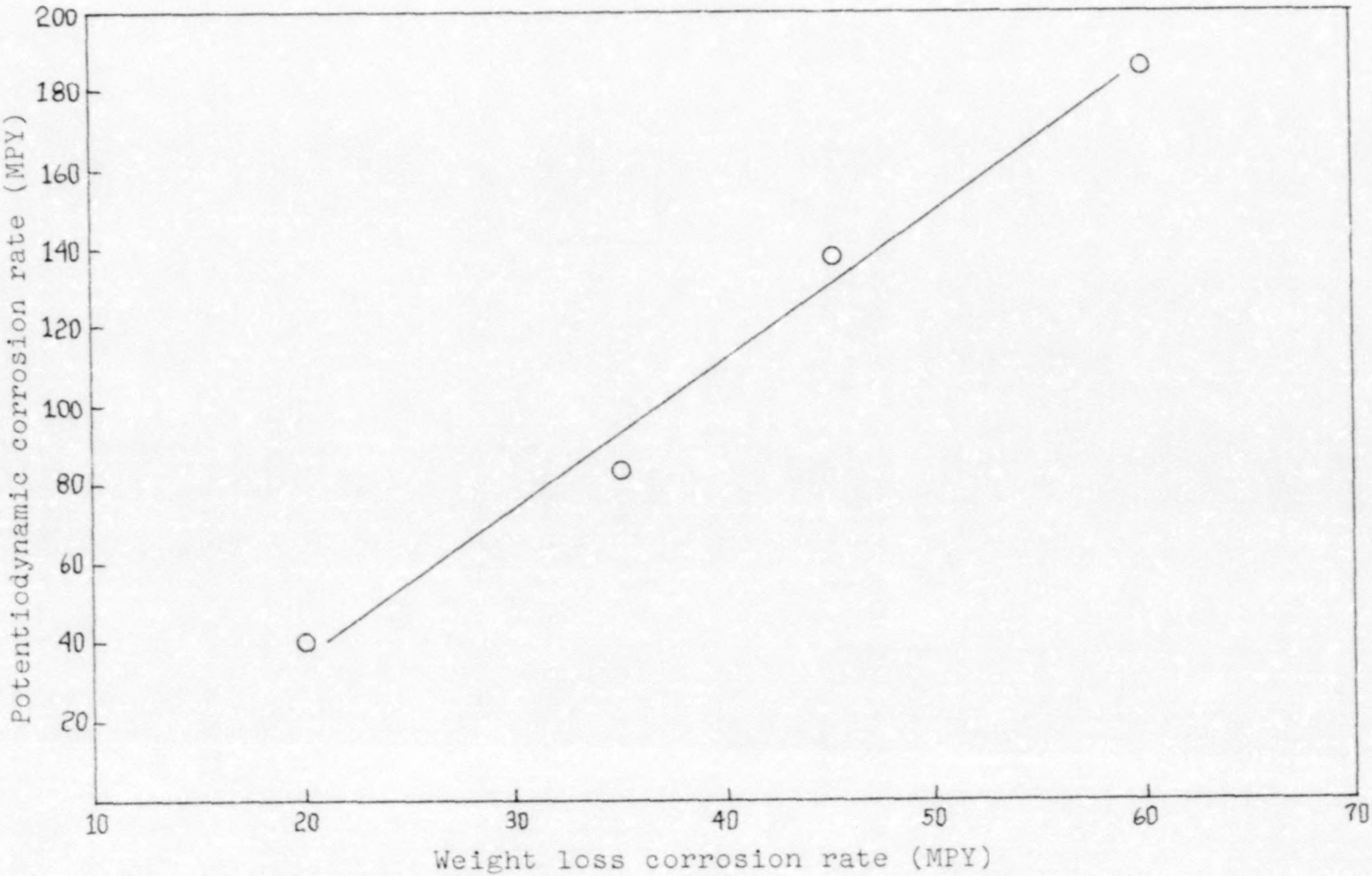

Figure 22. Potentiodynamic versus weight loss corrosion rates for static solutions of aniline hydrochloride (aerated).

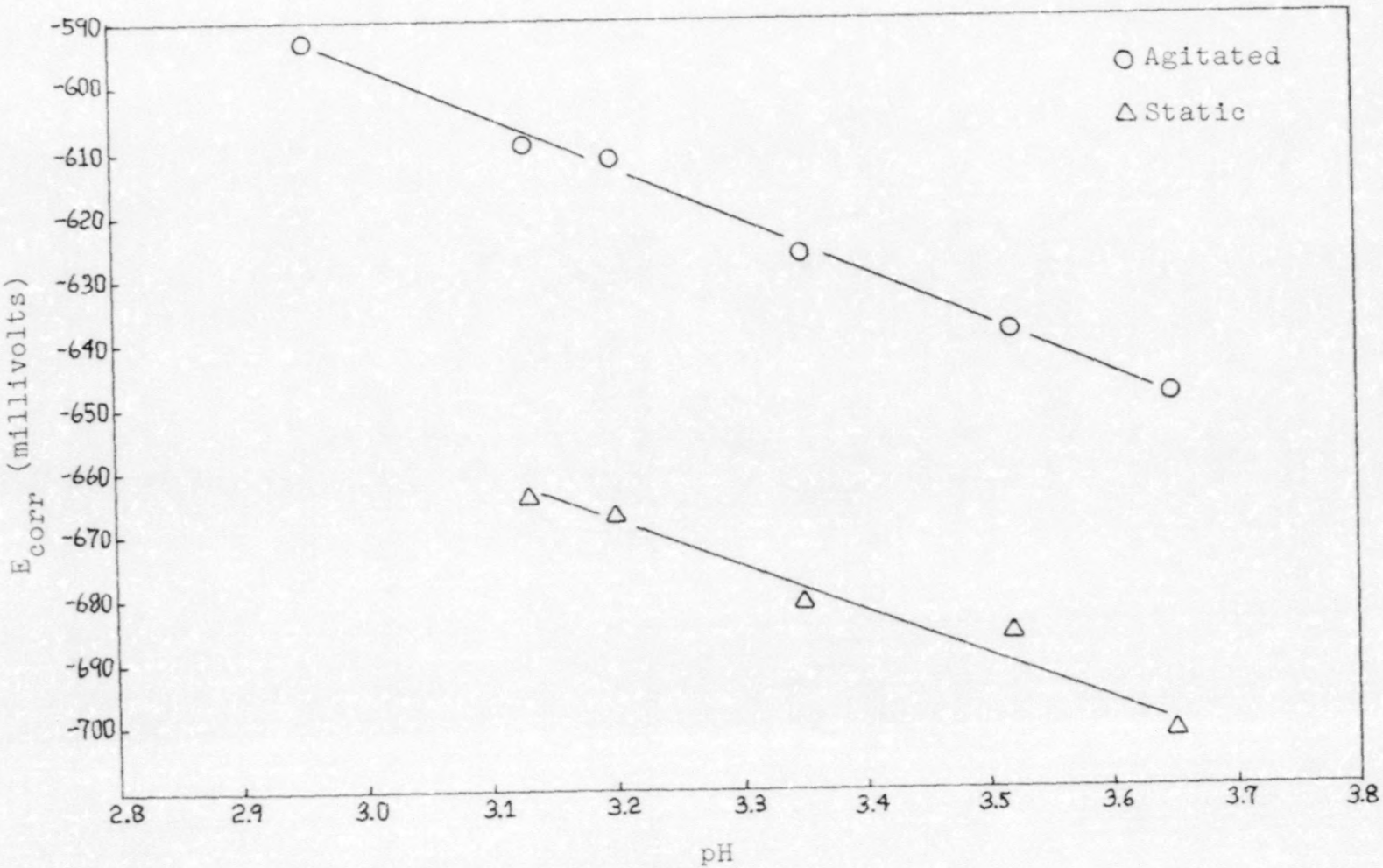

Figure 23. Dependence of E_{corr} on pH for cathodic curves (aerated).

pH as can be seen in the graph. Least squares fits of the data for both agitated and static modes are described by the equations, y = -80 x -356 and y = -70 x -445, respectively. Correlation coefficients for the data are 0.998 and 0.982, respectively. Kelly observed similar behavior for iron in acid sulfate solutions and interpreted it in terms of the kinetics of the hydrogen evolution reaction.[25]

It was mentioned earlier that cathodic and anodic intercepts at E_{corr} were displaced by an amount on the current coordinate which appeared to be a function of pH. The data are listed in Table 7 and represented in Figure 24. At low concentrations the cathodic values for I_{corr} are higher than the anodic values but the trend reverses between 400 and 800 ppm when the anodic values become higher than cathodic. The correlation coefficient for a least squares fit of the data is 0.988. An explanation for this behavior is not available but the correlation seems to be real.

Anodic values for I_{corr} and the equivalent calculated corrosion rate show good linear correlation with pH. A least squares fit of the data is given by the equation y = -1.6 x +2.2 with a correlation coefficient of 0.995. The data are illustrated in Figure 25. The anodic values do not show the decrease in calculated corrosion rate with decreasing pH as was possibly seen in the cathodic values, but instead show a consistent increase in calculated corrosion rate. This is what one might expect to see if no passivation or film formation occurred and the rate of the reaction was not diffusion controlled.

Table 7. (Log Ic_{corr} - Log Ia_{corr}) as a function of pH for aerated solutions.

Concentration Aniline hydrochloride (ppm chloride)	Log Ic_{corr}	Log Ia_{corr}	(Log Ic- Log Ia)	pH
200	-2.88	-3.43	-0.55	3.52
400	-2.77	-3.10	-0.33	3.35
800	-3.07	-2.85	+0.22	3.20
1000	-3.18	-2.82	+0.36	3.13
2000	-3.22	-2.51	+0.71	2.96

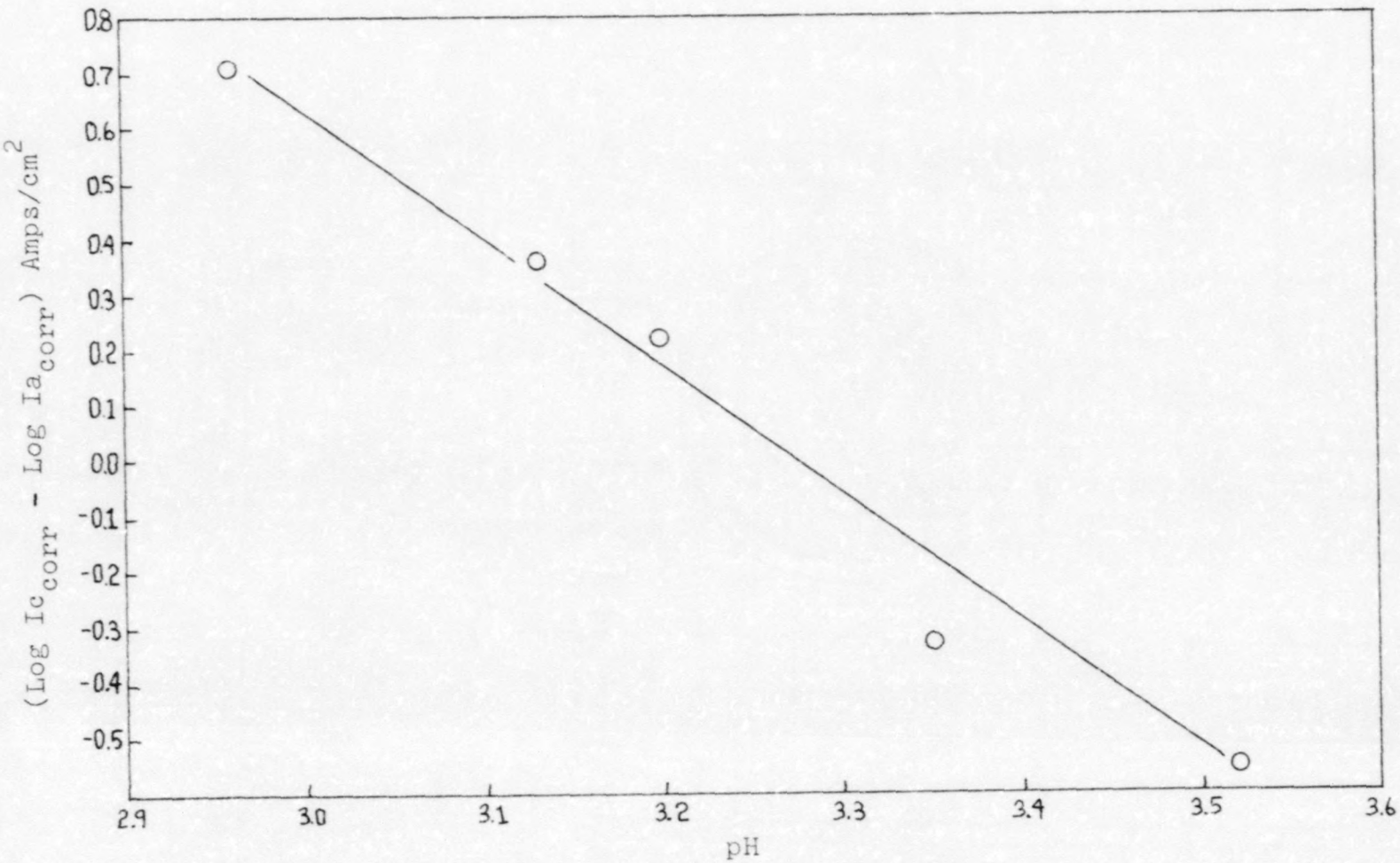

Figure 24. ΔI_{corr} versus pH for aerated solutions of aniline hydrochloride.

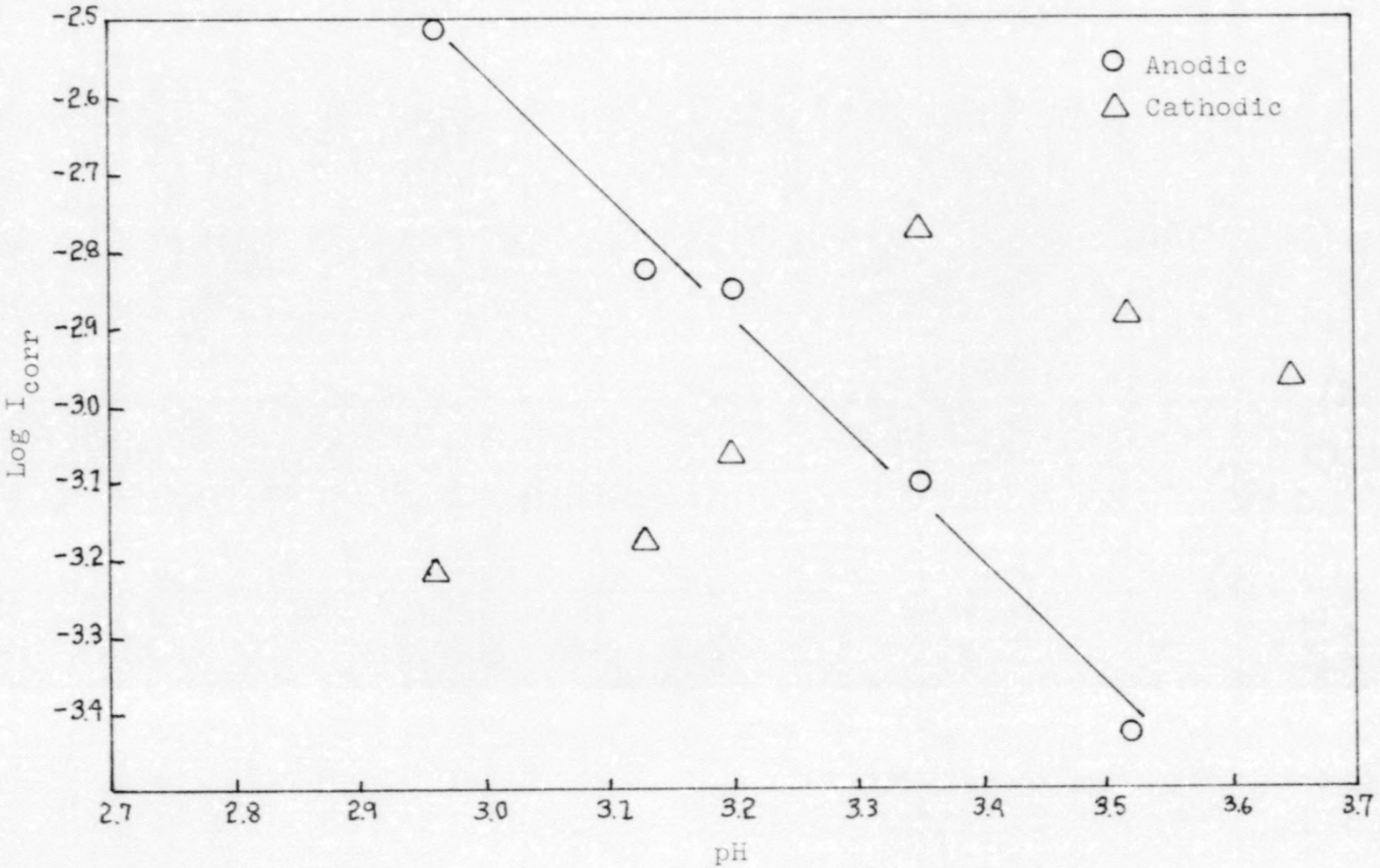

Figure 25. Log I_{corr} versus pH for anodic and cathodic curves (aerated).

Deaerated Solutions

One of the more interesting results from the potentiodynamic experiments is the behavior of deaerated 1000 and 5000 ppm chloride solutions. There appears to be two modes of corrosion corresponding to high and low corrosion rates in these systems. Data for the two series of experiments in deaerated 1000 and 5000 ppm chloride solutions are listed in Table 8. Tracings of the 1000 ppm data are shown in Figure 26 and for the 5000 ppm data in Figure 27. Several interesting observations can be drawn from the data.

In the deaerated systems initial corrosion rates calculated from cathodic scans were very low, in the order of 6 to 10 MPY, and remained low until an anodic scan was run. After the anodic scan the calculated corrosion rates increased markedly to values similar to those of aerated systems. Furthermore, the anodic scan exhibited a transition by suddenly breaking to higher anodic currents as the upward scanning potential reached about -520 mV versus SCE. This transition resembles discontinuity in anodic polarization reported by Kelly.[26] Calculated corrosion rates remained high until the specimen was removed from the solution and abraded with 400, followed by 600, grit silicon carbide paper. When the specimen was placed back into the solution, corrosion rates calculated from cathodic scans showed a consistent decrease with time until after a few hours corrosion rates were similar to those observed initially. This process could be repeated several times with the same result for both concentrations. In all cases corrosion rates did not increase

Table 8. Deaerated 1000 and 5000 ppm aniline hydrochloride solutions.

Concentration Aniline hydrochloride (ppm chloride)	Immersion Time (Hrs)	Cathodic/ Anodic	E_{corr}	Log Icorr	MPY
1000	4.00	Cat.	-655	-4.72	9
	4.30	Cat.[a]	-662	-4.60	11
	4.60	And.[a]	-651	-5.03	4
	4.90	Cat.	-634	-3.55	128
	4.92	Specimen resurfaced and replaced.			
	21.6	Cat.	-652	-4.63	11
	22.6	Cat.	-647	-4.69	9
5000	6.40	Cat.	-642	-4.91	6
	7.30	And.	-639	-5.10	4
	7.60	Cat.	-612	-3.21	280
	8.10	And.	-597	-3.36	198
	8.30	Specimen resurfaced and replaced.			
	24.3	Cat.	-640	-4.79	7

[a] Static solution

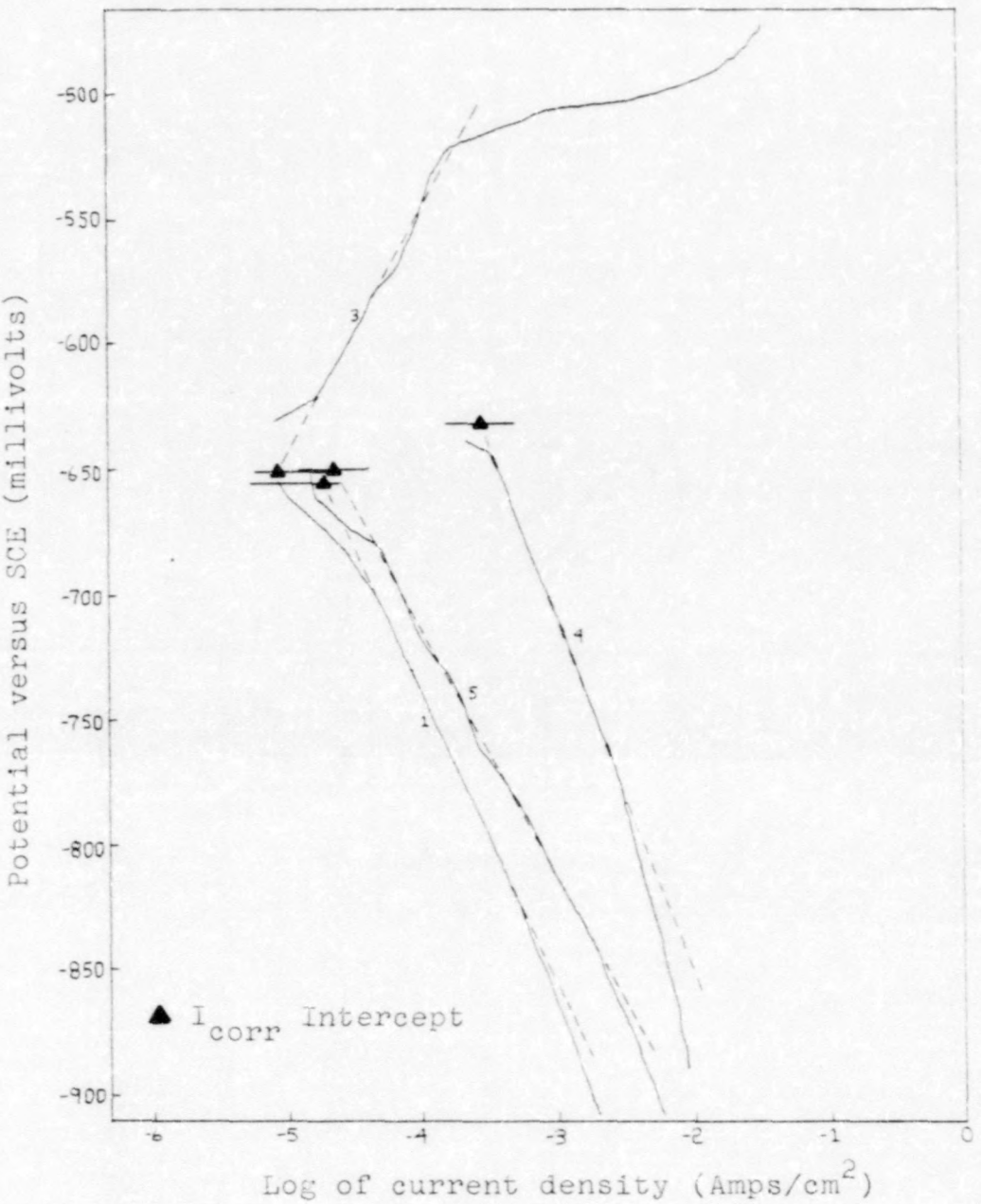

Figure 26. Potentiodynamic curves for deaerated 1000 ppm solution.

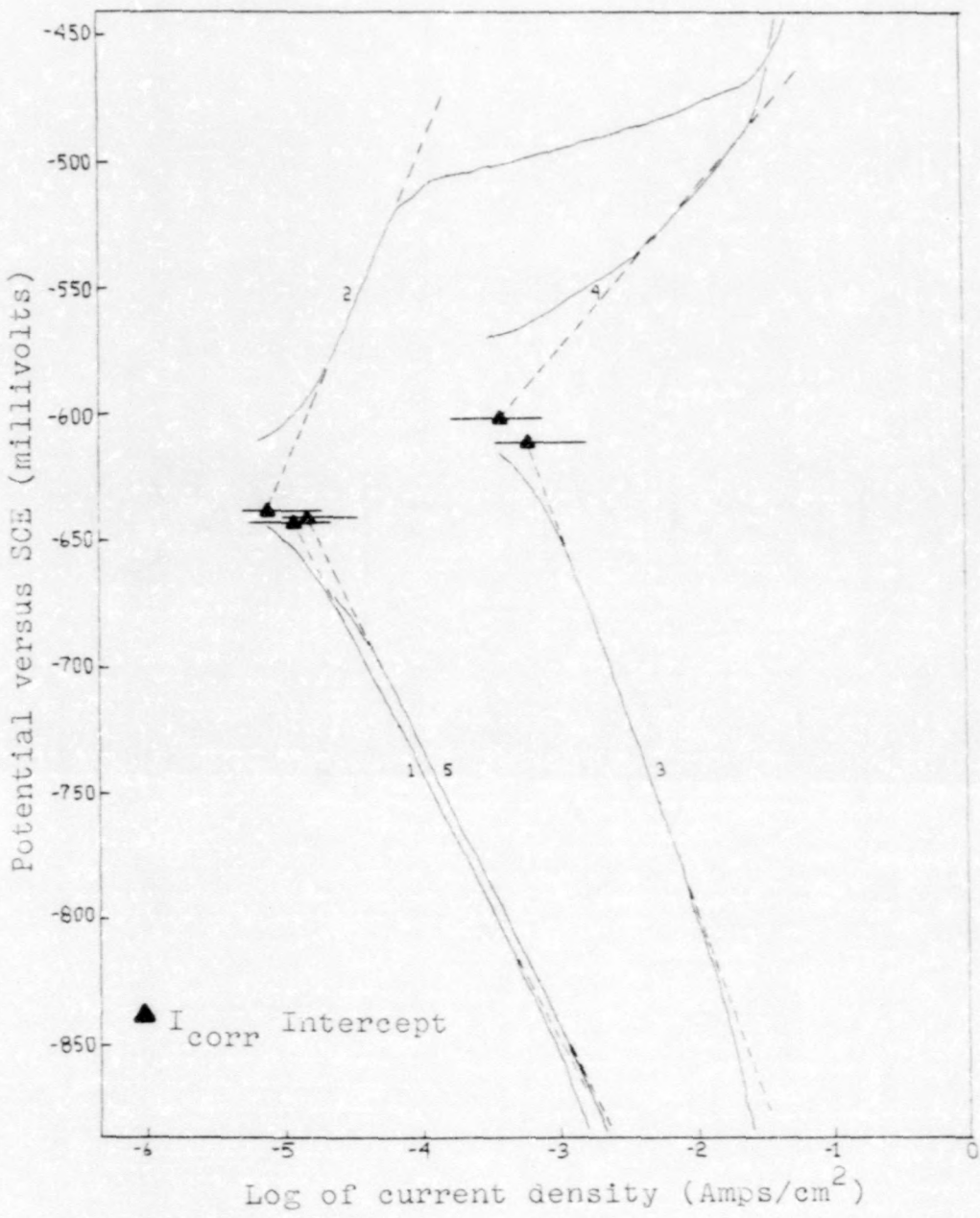

Figure 27. Potentiodynamic curves for deaerated 5000 ppm solution.

until an anodic scan was run which reached voltages above about -520 mV versus SCE. An anodic scan to voltages less than about -520 mV did not affect the calculated corrosion rates.

The surface of the specimen remained bright and untarnished for periods up to 16 hours in the low corrosion rate mode. During an anodic scan the surface would tarnish quickly and turn black when voltages exceeded about -520 mV. In reference to Figure 26, corresponding to a 1000 ppm solution, cathodic and anodic overvoltage curves 1 and 3, respectively, show the low corrosion rate mode and the atypical behavior of the anodic scan. Cathodic curve 2 listed in the Table but not shown in the Figure was obtained in static solution. Log I_{corr} values for agitated versus static are almost the same for the low corrosion rate mode, but the static curve showed more concentration polarization as evidenced by a steeper slope beginning at about -800 mV. Curve 4 was run after an anodic scan illustrating the high corrosion rate mode. After the specimen was resurfaced and replaced, corrosion rates dropped sharply as shown by curve 5. Curve 6, also not shown in the figure, was run after an anodic scan which did not exceed -520 mV. Curve 6 is practically identical to curve 5. This observation indicates that the high corrosion rate mode is not induced until voltages exceed about -520 mV.

Figure 27, corresponding to a 5000 ppm solution, shows the same behavior as the 1000 ppm solution. Corrosion rates begin low, sharply increase after an anodic scan, but then return to initial rates after resurfacing the specimen.

Introduction of more oxygen into the system by bubbling air through the solution also causes the curves to shift to higher currents and thus higher calculated corrosion rates. Almost immediately after air was introduced into the system the specimen began to tarnish and entered the high corrosion rate mode as evidenced by calculated corrosion rates from cathodic scans. This effect was observed even when an anodic scan was not run.

It was noted that the "break" in the anodic scan could also be observed in aerated solutions but to a lesser extent than deaerated solutions. Furthermore, the potential at which the break occurred was very consistent in all concentrations of aniline hydrochloride. The average value of the break for several concentrations ranging from 200 to 5000 ppm was -528 mV versus SCE with a standard deviation of 8.75 mV. The data are listed in Table 9. This result indicates that a critical potential must be exceeded in order for the corrosion rate to shift to the high rate mode.

An explanation for the behavior described above which is consistent with weight loss observations follows. The formation of a surface film is dependent on the concentrations of aniline hydrochloride and oxygen in the system. At low concentrations of oxygen the film is effective in reducing corrosion even though the system is capable of causing high corrosion rates. As oxygen concentration increases, the film becomes less stable and thus less effective. Anodic scans exceeding -520 mV versus SCE disrupt the film and alter

Table 9. "Break" potential for anodic scans of various concentrations of aniline hydrochloride (aerated and deaerated).

Concentration of Aniline hydrochloride (ppm chloride)	E_{corr}	"Break" Potential
200	-642	-538
200	-640	-533
425	-631	-533
450	-640	-520
1000	-608	-524
1000	-626	-520
1000	-651	-521
1100	-638	-540
1100	-652	-531
2000	-588	-512
2000	-595	-525
2000	-614	-534
5000	-639	-521
5000	-605	-539

the surface of the metal so that film formation does not reoccur. Resurfacing the specimen allows reestablishment of the film if the solution remains deaerated.

CONCLUSIONS AND RECOMMENDATIONS

The application of the potentiodynamic technique of corrosion measuring to the study of corrosion of carbon steel in aqueous aniline hydrochloride solutions simulating coal liquid wash waters has revealed several beneficial conclusions. These conclusions are directly applicable to the design of coal liquid wash water areas of commercial coal liquefaction plants. Furthermore, it was found that the potentiodynamic technique correlated with the more conventional weight loss technique. The conclusions derived from this study are as follows:

1) Potentiodynamic corrosion rates calculated from cathodic polarization experiments correlate with weight loss corrosion rates.

2) Corrosion of carbon steel M1044 in aerated aqueous solutions of aniline hydrochloride is velocity dependent.

3) High concentrations (i.e. 1000 ppm) of aniline hydrochloride tend to cause lower corrosion rates than low concentrations (100 ppm).

4) Decreased corrosion rate with increasing concentration of aniline hydrochloride can be attributed to the formation of a surface film.

The bimodal behavior of corrosion in deaerated aniline hydrochloride solutions should be studied in more detail. This observation could be extended to the study of organic

corrosion inhibitors which form surface films. Further investigations with the potentiodynamic technique could be simplified by the use of a rotating disc electrode which would reduce the effect of diffusion and thus reduce concentration polarization. This would permit a closer look at the activation polarization curves.

BIBLIOGRAPHY

1. Berkowitz, N., An Introduction To Coal Technology, p. 18, Academic Press, New York, NY (1979).

2. Davis, B., et. al., Coal Liquids Distillation Tower Corrosion: Synergeistic Effects of Chlorides, Phenols and Basic Nitrogen Compounds. I&EC Process Design and Developement, 22, p. 15, (1983).

3. Boykin, G., Personal Communication, (1979).

4. Saques, A., B. Davis, Mechanisms of Corrosion And Alloy Response In Coal Liquid Systems Containing Chlorides, Proceedings of the NACE Corrosion Conference, Berkely, CA, (1982).

5. Lewis, H., et. al., Monthly Technical Progress Report, FE-2270-50, June (1979).

6. Canfield, D., S. Iharra, J. McCoy, Hydrocarbon Processing, 59(7), p. 203, (1979).

7. Davis, B., Thomas, G., A. Saques, Fuel Processing Technology, 8, pp. 77-93, (1983).

8. Thomas, G., M. Margolis, B. Davis, Submitted to Fuel Processing Technology.

9. Jewitt, C., Presentation at the Workshop on Corrosion/ Errosion in Coal Liquefaction Pilot Plants, Oak Ridge, TN, Nov 29, (1979).

10. NACE Task Group T-30-1, Modern Methods for Determining Corrosion Rates, NACE Publication 3D170.

11. Stansbury, S., Fundamentals of Corrosion, Dept. of Chemical, Metallurgical and Polymer Engineering, University of Tennessee, (1983).

12. Adamson, A., A Textbook of Physical Chemistry, Academic Press, New York, NY, (1973).

13. Copson, H., Ind. Eng. Chem., 44, p. 1745, (1952).

14. Tafel, J., Z. Phys. Chem., 50, p. 641, (1905).

15. Stearn, M., A. L. Geary, Electrochemical Polarization I. A Theoretical Analysis of the Shape of Polarization Curves, J. Electrochemical Society, 104, pp. 56-63, (1957).

16. Wagner, C., W. Traud, The Interpretation of Corrosion Phenomena by Superimposition of Electrochemical Partial Reactions and the Formation of Potentials of Mixed Electrodes, Z. Electrochem., 44, pp. 391-402, (1938).

17. Stern, M., Fundamentals of Electrode Processes in Corrosion, Corrosion, 13, pp. 775-782, (1957).

18. Nathan, C.C., Corrosion Inhibitors, NACE, Houston, TX, p. 1-6, (1979).

19. Hackerman, Macrides, Corrosion, 18, p. 332, (1962).

20. Hamner, N.E., Corrosion Data Survey, 5th Edition, NACE, Houston, TX, (1974).

21. Hoyt, S.L., ASTM Handbook Metal Properties, McGraw Hill Book Co. Inc., New York, NY, (1954).

22. Saques, A.A., Personal Communication, (1984).

23. Kubaschewski, O., B.E. Hopkins, Oxidation of Metals and Alloys, Butterworths, London, England, (1962).

24. Stern, M., The Electrochemical Behavior, Including Hydrogen Overvoltage, of Iron in Acid Environments, J. of the Electrochemical Society, pp. 609-616, Nov., (1955).

25. Kelly, E.J., The Active Iron Electrode I., J. of the Electrochemical Society, pp. 124-131, Feb., (1967).

26. Kelly, E.J., The Active Iron Electrode II., J. of the Electrochemical Society, pp. 1111-1119, Nov., (1968).